Abstract

Title:	**DESIGN AND ANALYSIS OF NEW GASIFICATION APPARATUS BASED ON THE STANDARD CONE CALORIMETER**
	Xuan Liu, Master of Science, 2012
Directed By:	**Professor Stanislav I. Stoliarov**
	Department of Fire Protection Engineering

A simple, inexpensive, safe version of pyrolysis apparatus is developed base on the standard cone calorimeter (ASTM E 1354). A controllable oxygen concentration (0% to 21% by volume) environment in the vicinity of 80 mm by 80 mm square sample positioned under the cone radiant heater is achieved by means of "Controlled Atmosphere Pyrolysis Apparatus". Valid gasification mass loss rate measurements have been obtained for both poly(methyl methacrylate) (PMMA) and polypropylene (PP) samples under external heat fluxes of 35kW/m^2 and 50kW/m^2. Reasonable value of thermal conductivity for PMMA is measured. With the thermal conductivity and parameters defined by Differential Scanning Calorimeter (DSC) of PMMA, the gasification mass loss rate is well simulated using Thermo-Kinetic Model of Burning (ThermaKin).

DESIGN AND ANALYSIS OF NEW GASIFICATION APPARATUS BASED ON THE
STANDARD CONE CALORIMETER

By
Xuan Liu

Thesis submitted to the Faculty of the Graduate School of the
University of Maryland, College Park, in partial fulfillment
of the requirements for the degree of
Master of Science
2012

Advisory Committee:
Professor Stanislav I. Stoliarov, PhD, chair
Professor James G. Quintiere, PhD
Professor Marc R. Nyden, PhD
Professor Peter B. Sunderland, PhD

Acknowledgements

I would like to thank everyone I know in my Master's program. All the help, passion, encouragement, knowledge gained from the experiences with them were playing an important role in this study.

Dr. Stanislav I. Stoliarov, my advisor, surely deserves the most significant acknowledgement. I would like to thank him for trusting me, sponsoring me and admitting me as a research assistant in this great group. I'm deeply grateful to his patience and instructions from the very beginning of this project. I could hardly imagine how I could solve some of the hard problems and make progresses in this study if without his knowledge, encouragement and patient guidance. The time, energy and passion he has been dedicating to this project are also the most encouraging in my Master's program. There were several times I felt frustrated by the complicated problems in this study, but Dr. Stoliarov could always use his deep understanding of the project and experience to lead this project back on track. I feel so lucky being in his group, and even luckier that I will stay in this group with Dr. Stoliarov for the Ph.D program.

I appreciate the great help from Dr. Kashiwagi, Dr. Steckler and Dr. Nyden. They provided me the great chance of using the NIST Gasification Apparatus to get the valuable reference measurements for the design in this study.

I also would like to thank Olga. She has been really helpful when I was doing experiments in the lab. If I met some problems in the lab and couldn't find the solution, "where is Olga?" is always the first question come into my mind. Mollie also

deserves big acknowledgement in this study, she helped a lot of experimental work, and I appreciate her time of editing my thesis. I hope she will do a great work in her project.

Last but not least, I would like to thank my family. My parents have been giving me a lot of encouragement from China. More importantly, special thanks should be delivered to my wife, Yikang Gu. I would like to appreciate her huge contributions to our newly built family during the past two years. She has given up a lot of her own time and been dedicating a lot to our small family. This project is surely more nicely done because of her. Thank you, Kangkang.

Contents

List of Tables

List of Figures

1. Introduction

1.1 The Pyrolysis Problem

Computational fire modeling has been focused on by the fire protection community for several decades, in part because of the economical advantage the modeling has over conducting fire tests. Recently, a significant effort has been made to develop detailed, continuum models of pyrolysis or burning for combustible materials. These models, capable of accurately predicting the detailed processes that take place in the condensed phase of a burning material play an essential role to produce accurate predictions with Computational Fluid Dynamics (CFD) codes. Pyrolysis models compute the rates of gaseous fuel generation by solid material samples exposed to external heat. These models require definition of input parameters such as physical and chemical properties of the material components. One major obstacle for the modeling to produce accurate predictions is the lack of material-specific properties and the difficulties of measuring these parameters.

The current study will address this problem by means of gasification experiments on testing materials. Gasification experiments allow a flat plaque of a combustible material to be subjected to a uniform external heat flux, while the mass of the sample is recorded as a function of time, in a non-oxidizing or partially-oxidizing atmosphere. The primary difference between the gasification experiments and a standard cone calorimeter test is that, in the gasification experiments, due to the lower oxygen concentration, the ignition of a combustible material is prevented. Without the

additional heat flux from the flame usually happening in a normal cone calorimeter test, gasification experiments are able to provide excellent means for a quantitative analysis of the thermal degradation thermodynamics and energy transport inside the material.

The main purpose of the current study is to develop an inexpensive, simple and safe version of gasification experiment apparatus based on the standard Cone Calorimeter. This will finally not only give a methodology for measurement of thermal conductivity of a certain material, but also provide a way of validation for continuum burning models.

1.2 Early Studies on Controlled Atmospheric Cone Calorimeter

Cone Calorimeter, which was developed in the early 1980s, has been recognized as one of the most significant bench-scale instruments for fire testing. It was developed as a research test by Babrauskas at NBS. The name of cone calorimeter derives from its truncated cone shaped radiant heater. The basic apparatus is described in reference [1]. Within several years, the cone calorimeter has been quickly accepted as standard test such as ASTM E 1354 [2] and ISO 5660-1 [3].

The cone calorimeter tests are designed to evaluate the fire behavior of a chosen material (normally a 100mm by 100mm square) under well-ventilated and fully developed fire scenarios. In these tests, important measurements can be taken such as the mass loss rate (MLR), heat release rate (HRR), smoke obscuration, and any typical n products of combustion and decomposition, specifically carbon dioxide and carbon monoxide. Therefore, cone calorimeter tests are usually used as a universal approach to

rank and compare the fire behavior of different materials of interest. It is then not surprising that the cone calorimeter is adopted as one of the most commonly used characterization tool in the fire and material research.

However, one disadvantage of the standard cone calorimeter tests is that only well-ventilated (fuel-lean or oxygen rich) conditions can be tested due to the open atmospheric design. A more realistic fire scenario is normally oxygen-rich in the early stage of fire growth and becomes oxygen-lean at the fully-developed stage of fire later on. Therefore, one of the main criticisms for the standard cone calorimeter design is that it is not able to measure the material properties in the most realistic fire scenarios. When it is well ventilated, measurements such as mass loss rate, heat release rate and yield of carbon dioxide will reach the maximum value, while measurement such as the yield of carbon monoxide or smoke will be under-estimated. The evaluation of a certain kind of material, therefore, will not be sufficiently accurate.

To be able to evaluate the fire or degradation behaviors of materials under non-ambient atmospheric conditions, some modifications of cone calorimeter have been developed. One of these is the controlled atmosphere cone calorimeter (CACC) introduced by the work [4-7]. Numerous researchers have adopted this device and have conducted studies in reduced oxygen environments [8-11]. Leonard et al. also introduced a version of CACC in their study [12]. Kashiwagi et al. designed a modification of a standard cone calorimeter to control the local oxygen concentration at the testing material, by installing a duct over the sample under the cone heater to direct high purity

nitrogen parallel to the sample surface [13]. In another study by Kashiwaigi, a controlled atmosphere cone calorimeter was developed to understand the effect of oxygen on non-flaming transient gasification of polymers [14]. One of the oxygen concentrations of interest in this study is as high as 40%, but the flaming was stopped by separating the cone heater (source of ignition) and the heated samples. One other example of the gasification apparatus is the one developed by Austin et al. in 1997 at NIST [15]. Studies have used this apparatus to obtain important gasification experiment data [16]. The FM Global has been working on a research apparatus called FM Global Fire Propagation Apparatus. This apparatus is described in reference [17].

The similarity between these previous designs is that a chamber is installed around the sample. The installed chamber results in some disadvantages. First, as the chamber heats up, the re-radiation from the chamber causes extra radiant heat flux to the sample. Even if the chamber is paint black, this extra heat flux is not able to be totally removed. Second, water cooling system to reduce the re-radiation from the chamber to sample (such like the NIST gasification cone calorimeter) increases the cost. Last but not least, there is a potential safety problem with the enclosed chamber as explosions may sometimes occur if operation is not proper. The gasification apparatus developed in this study, however, does not have these disadvantages. This is also one of the main motivations of this study.

1.3 NIST Gasification Apparatus

Among all those previous studies, one of the most representative implementations of gasification tests is the NIST Gasification Apparatus developed by Austin et al. [15]

A picture and an illustration of this apparatus are shown in Figure 1.
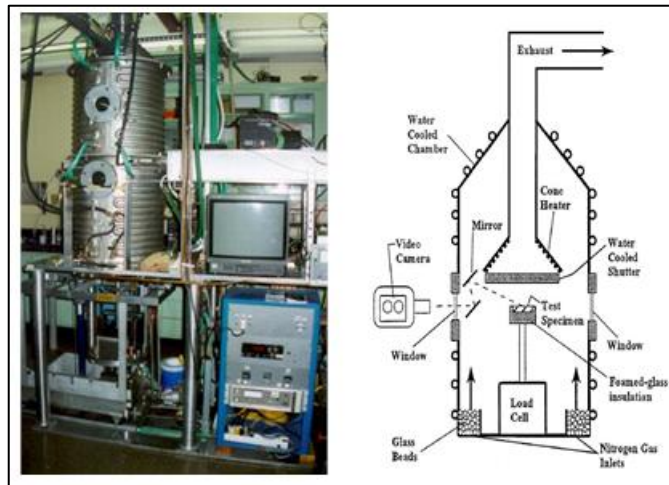
Figure 1. NIST Gasification Apparatus

This NIST Gasification Apparatus consists of a stainless-steel cylindrical chamber. The chamber is 1.70m high and 0.61m in diameter. To remove the re-radiation from the chamber, the inner wall of the chamber is painted black and the whole chamber is cooled down to the room temperature (25°C) by the water cooling system. Nitrogen is introduced from the bottom of inside the chamber. Glass beads are packed right above the inlet of the nitrogen to ensure a uniformly nitrogen flow being evenly delivered into the chamber. An exhausting system is present above the cone heater to remove the gasification products from the chamber. A load cell placed on the removable bottom plate is used to record the mass changes during the gasification tests. The bottom plate of the apparatus is removable to allow the sample to be placed on the load cell when

the bottom plate is taken off from the chamber. The sample can be introduced into the chamber by putting the whole bottom plate back to the chamber. After the sample is placed in, the whole chamber will be tightly sealed. Then 1,200 SLPM of high purity nitrogen is pumped into the chamber to purge the chamber of oxygen. An oxygen probe is placed around the sample to show the volumetric concentration of oxygen inside the chamber. When the oxygen is reduced to 0%, the water-cooled shutter in between the cone heater and sample is removed and the gasification test begins. Video could be taken from the observation windows as shown in Figure 1.

There are several differences between the NIST Gasification Apparatus and a normal cone calorimeter. First, the cone heater used in this apparatus is 30cm in diameter, which is bigger than the heater in a normal cone calorimeter. Second, this cone heater is set at a constant temperature (808°C), which will ensure the same spectral distribution at all flux levels. Third, the heat flux of interest is achieved by adjusting the distance of the sample from the heater while in the normal cone calorimeter it is achieved by adjusting the temperature of the cone heater.

Several gasification tests were executed in this apparatus on PMMA and PP. The tests were under heat fluxes of interest in this study (35kW/m^2 and 50kW/m^2). These tests have given valuable reference data for the designs in this study.

1.4 Thermal Kinetic Model of Burning (ThermaKin)

The fact that there is lack of a quantitative understanding of the relationship between the results of various materials fire tests used in this field is a main obstacle in developing more effective passive fire protection. Multiple testing techniques are needed because of the complexity of fire phenomena and their sensitivity to environmental conditions. Many applications for which fire safety is a concern require development of a new test that mimics the most probable fire scenario. With few exceptions, these tests are expensive to build and operate. They also usually require a significant amount of material. A one-dimensional numerical pyrolysis model called ThermaKin (developed by Dr. Stanislav I. Stoliarov and Dr. Richard E. Lyon) [18] is utilized to address this problem.

ThermaKin is a flexible computational framework that solves energy and mass conservation equations, which are formulated in terms of rectangular finite elements. It is a powerful computational tool that predicts the behavior of materials exposed to fire. The goal of the model is to considerably reduce the number and complexity of the tests necessary for a comprehensive characterization of the materials of interest. The foundation of the tool is a mathematical model that describes transient thermal energy transport, chemical reactions, and the transport of gases through the condensed phase. The model also captures important aspects of a material's behavior such as charring and intumescence. The details of ThermaKin are described elsewhere [18]. The model has been validated studies on both charring and non-charring materials [19, 20].

In this study, after the gasification apparatus is developed and validated, ThermaKin is utilized to estimate the thermal conductivity of a certain material by simulating the temperature profiles of material while the material is being gasified. This will be introduced in Section 4. Finally, the predictive power of ThermaKin and validity of its parameters will also be verified against the results of gasification experiments.

1.5 Materials of Interest

Two very commonly used non-charring polymers, Poly(methyl methacrylate) (PMMA) and Polypropylene (PP), are the object of focus in this study. Both materials are 6mm thick. They are cut into samples of size of 80mm by 80mm. The information about both materials is listed in Table 1.

Table 1. Information of Testing Materials

Plastic	Trade Name	Manufacturer	Distributor
PMMA, Poly(methyl methacrylate)	ACRYLITE FF Acrylic Sheet	CYRO Industries	Evonik Industries
PP, Polypropylene	Protec HPP (Homopolymer Polypropylene)	Compression Polymers Corp	U.S. Plastic Corp

The PMMA used in this study is colorless with light transmittance of 92%. The PP used in this study is white-tan. Figure 2 shows both materials.

To make sure that the testing samples can be well contained during the tests, aluminum foil is used to wrap around the sides as well as the bottom of the sample before each test. Only the top surface is not covered by aluminum foil thus exposed to

the external radiant heat flux. To ensure one-dimensional heat transfer inside the testing samples, the samples are placed into a 80mm by 80mm (size of the sample) square opening.in the center of a piece of 100mm by 100mm Kaowool.
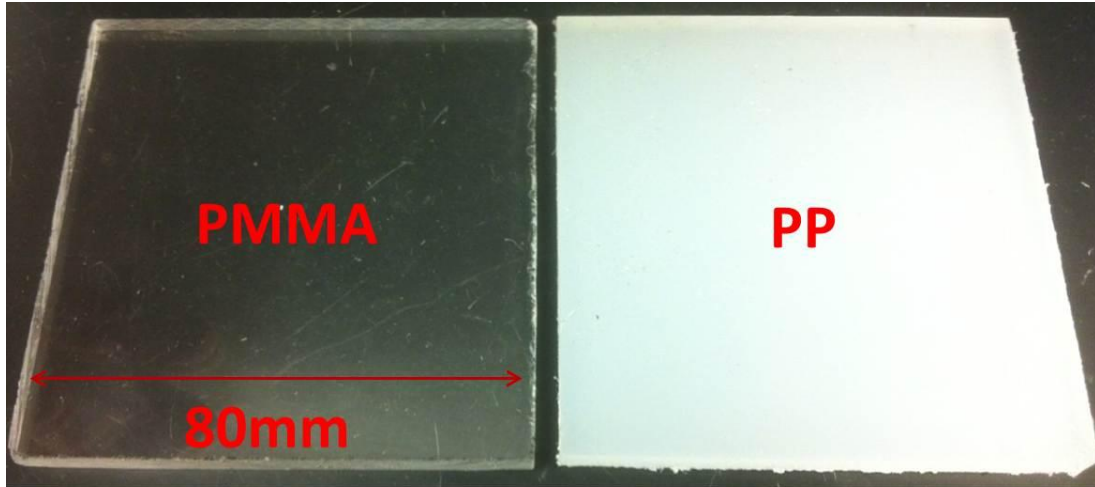
Figure 2. Materials of Interest

1.6 Objective of This Study

The whole process of this project and the objectives of this study are shown in Figure 3.
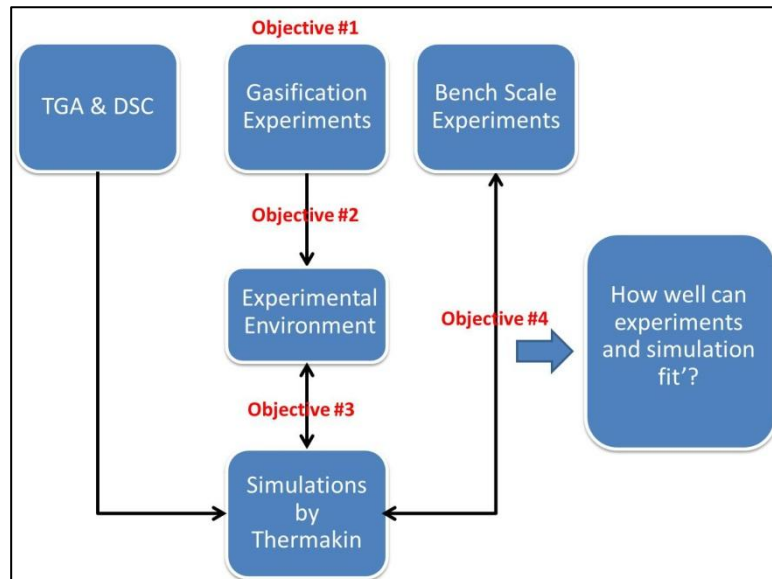
Figure 3. Objectives of This Study

The first objective of this study is to develop a gasification apparatus which will be able to reduce the oxygen concentration at the sample material under the cone heater in order to prevent the auto-ignition of the material of interest. This will give a very well-defined heat transfer boundary condition at the surface of the sample material without the additional heat flux from the flame that is observed in a normal cone calorimeter test.

The second objective of this study is to analyze the detailed experimental environment during the gasification tests. Since the design of a gasification apparatus in this study has brought in some other influencing factors (i.e. convective heat loss, measurement noise, oxidation factor), a detailed analysis needs to be conducted to understand these factors.

The third objective of this study is to find a method to estimate the thermal conductivity (k) value of a combustible material. In this study, ThemaKin simulations and the measurements of the back layer temperature of a combustible material are combined to give an estimation of materials of interest.

The fourth objective of this study is to verify the predictive power of ThermaKin and the measurements of properties of materials of interest by simulating the one-dimensional gasification experiments. With all properties measured either by TGA/DSC tests or estimation from gasification experiments and ThermaKin simulations, the gasification mass loss rate will be able to be simulated.

Upon completing the objectives stated above, a systematic methodology of parameterization and validation of continuum burning models will be developed. Further study will be focused on other combustible materials and the construction of a database containing all material-specific properties.

2. Gasification Apparatus Design - "Nitrogen Frame"

Efforts are made to design and construct a simpler and less expensive version of gasification apparatus based on the cone calorimeter we have in the lab. The challenges in this design include: 1). It is an open atmospheric environment. The whole system will be exposed to the ambient air and nitrogen will be flowed around the sample to create a very low oxygen concentration environment. It is challenging to make sure that the dilution of air made by high purity nitrogen around the sample is not only stable but also effective. 2). The dilution of air by nitrogen may cause problems, including convective heat loss and measurement noise etc. 3). As the oxygen is diluted instead of being totally removed around the sample, there would still be some oxidation factors, leading to uncertainties in the measurements.

In this first version of gasification apparatus – the "Nitrogen Frame", the main focus is concentrated on how to overcome all those challenges. Although it fails to solve all these problems, helpful experiences have been gained. These experiences lead to a much better version of gasification apparatus – "Controlled Atmosphere Pyrolysis Apparatus" CAPA- which is introduced in Section 3.

2.1 The Original Apparatus Design

In this first design, the air at the sample is being diluted by means of a "nitrogen frame" mounted around the perimeter of the 80mm by 80mm sample under the cone heater. The frame consists of four piece of stainless steel tube of 3/8" OD on each side and 40 very small orifices on each tube. The local oxygen concentration at the sample will be largely reduced by delivering a certain amount of high purity nitrogen (Airgas

HP300 N2) from the orifices along the stainless steel tubes on the frame to the surface

of the sample. This design is illustrated in Figure 4.

(a)

(b)

(c)

(d)
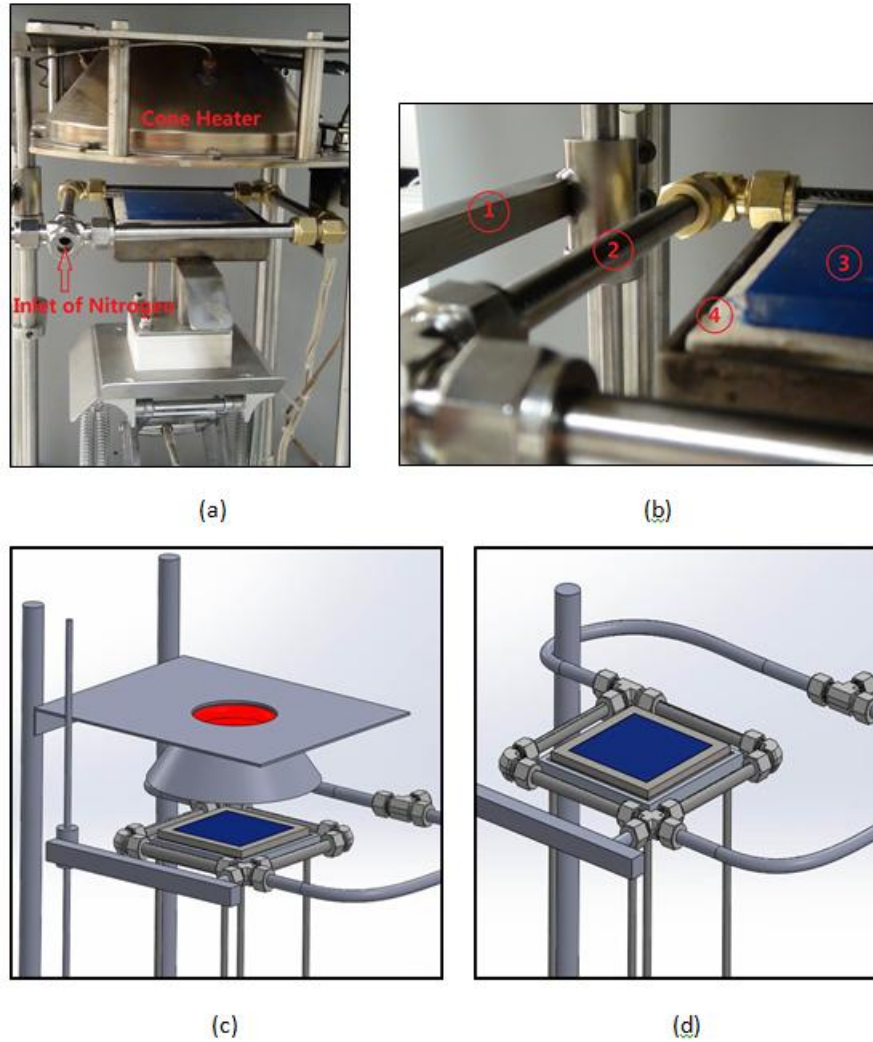
Figure 4. (a)Overview of the Design. (b)Detailed Picture: 1.Nitrogen Frame Holder. 2.Stainless Steel Tubes with Multiple Orifices. 3.Sample. 4.Kaowool. (c),(d) More Illustrations

2.2 Initial Gasification Mass Loss Rate Measurement

Figure 5 shows a more detailed section view of the Nitrogen Frame Gasification

Apparatus Design.
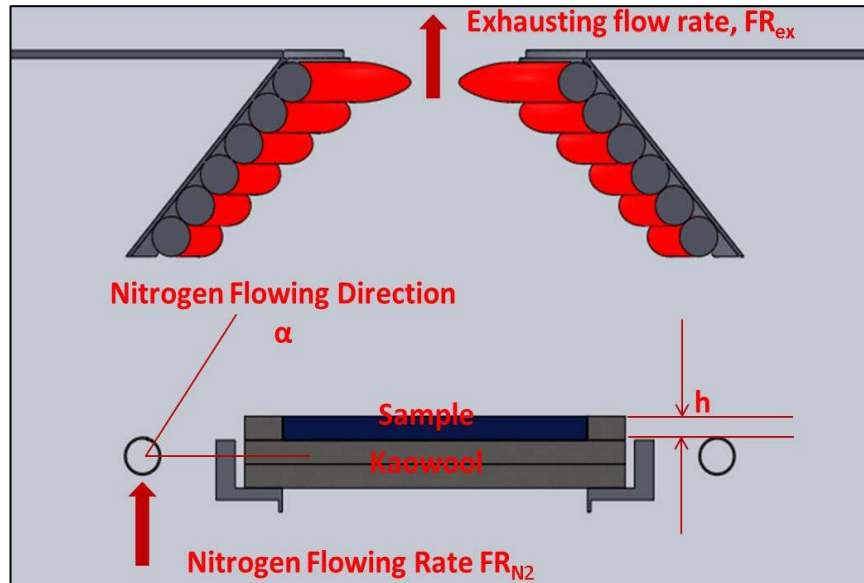
Figure 5. Detailed Section View of the Nitrogen Frame Design

The following are important parameters related to the settings of this design. 1).

The direction in which the nitrogen is flowing out from the orifices on the tube frame, α.

It is an angle relative to the horizontal level. 2). The nitrogen flow rate coming into the

tube frame, FR_{N2}. It is in of the unit of standard liters per minute (SLPM). 3). The relative

height from the upper edge of the tube frame to the surface of the sample, h. It is of the

unit of millimeters. When h>0, it means the upper edge of the tube frame is above the

level of the sample surface level. When h<0, it means the upper edge of the tube frame

is below the level the sample surface level. 4). The exhausting flow rate, FRex. It is of

24L/s.

All these parameters are important to understand how the apparatus works. For example, FR_{N2} determines how well the air around the sample could be diluted by nitrogen. The nitrogen temperature flow could greatly affect the convective heat loss from the sample. The flow rate of nitrogen (FR_{N2}) should not be too large or too small. If it is too large, the convective heat loss and the measurement noise will be very high. If it is too small, the oxygen concentration will not be reduced to the level where the auto ignition of the sample is prevented under the radiant heat flux from the cone heater. The angle of the nitrogen flow α is also playing a crucial role in this case since it not only affects the convective heat loss but also creates significant measurement noise for the mass loss rate. The exhausting flow rate, FR_{ex}, is important because it also has some influence on how low the oxygen concentration will get. It also helps to prevent the gaseous decomposition products from coming out during the gasification of polymers. The relative height, h, also influences the performance of this apparatus. Efforts were undertaken to try to find the optimal combination of all these parameters listed above.

Under an external radiant heat flux of 50kW/m^2, with a FR_{N2} of 100 SLPM, an h of -20mm, a FR_{ex} of 24 L/s, and a α of 40°, the auto ignition of a PMMA sample is stopped. The initial gasification mass loss rate measurement was recorded on a piece of PMMA sample using this apparatus. The data is shown in Figure 7.

Under the same heat flux of 50kW/m^2, a reference mass loss rate profile is obtained by using the NIST gasification apparatus for PMMA of the same size (80mm by 80mm). It is shown in the Figure 6.
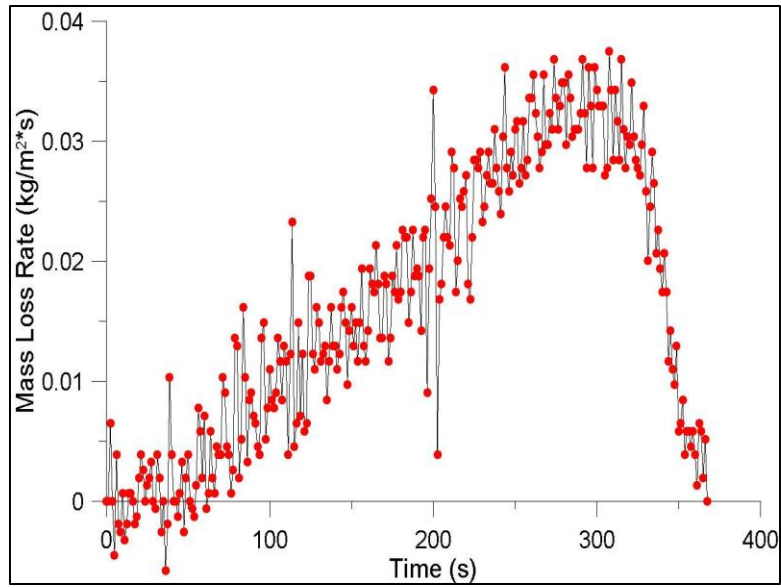
Figure 7. The Initial Gasification Mass Loss Rate of PMMA under 50 kW/m^2 by "Nitrogen Frame"
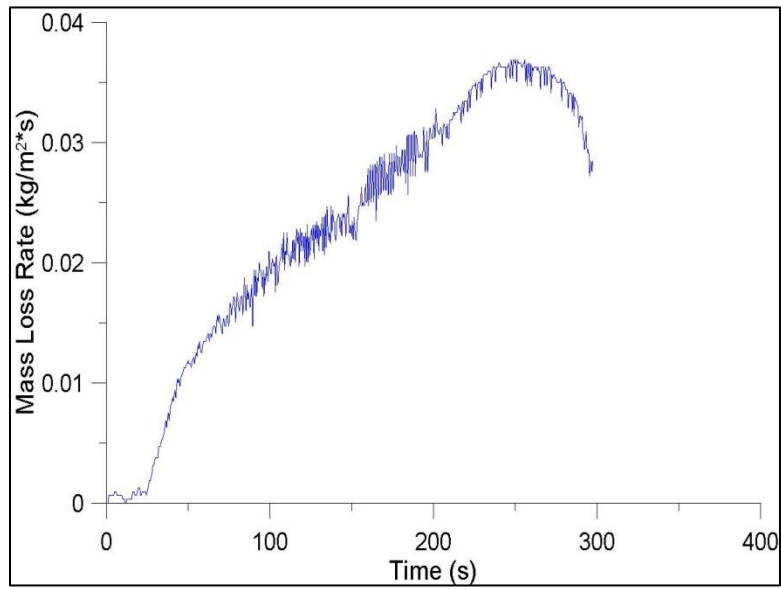
Figure 6. The Gasification Mass Loss Rate of PMMA under 50kW/m^2 by the NIST Gasification Apparatus

2.3 Mass Loss Rate Comparison.

These two mass loss rate measurements are compared to each other then. At first glance, the results appear to be closely correlated. The shape of the mass loss rate profile follows the same pattern as the one by the NIST apparatus. The peak values of the mass loss rate as well as the gasification times are also very close to each other. However, a closer comparison reveals several problems brought by the "nitrogen frame" gasification apparatus as shown in Figure 8.
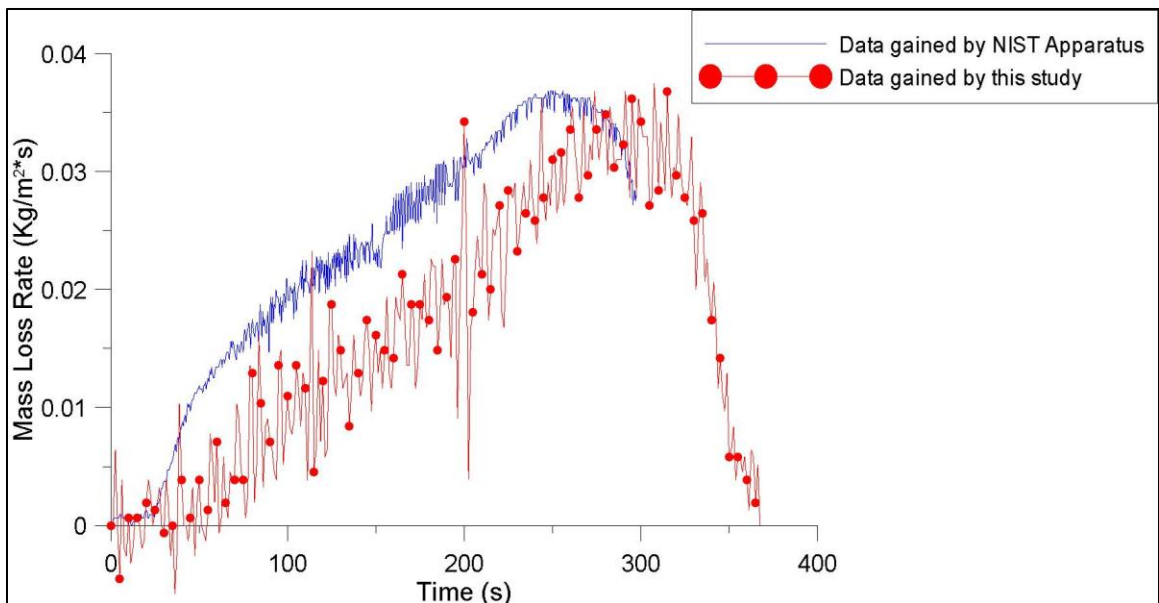
Figure 8. Comparison between MLR (NIST and "Nitrogen Frame" Apparatus) of PMMA under 50 kW/m^2

From the comparison in the plot above, there are two main differences between the reference data and the data obtained in this experiment. 1). The mass loss rate data measured by the "nitrogen frame" in this study is much more noisy than the one measured by the NIST gasification apparatus. 2). The mass loss rate date measured by the current study is generally lower than the one got from the NIST apparatus.

The explanation for these differences is evident. There are two principal reasons. First, even though the 100 SLPM of nitrogen flowing out from the tube frame and the orifices is not as large as the flow rate of nitrogen used in the NIST gasification apparatus (1,200 SLPM), the nitrogen in this apparatus is flowing onto the sample more directly. In the NIST apparatus, the nitrogen is uniformly distributed from the bottom of the chamber to the sample. In this study, the nitrogen is more or less directly flowing to the sample and covering the sample. Additional pressure onto the sample holder is significantly higher than those in the NIST gasification chamber. This flow causes a significant amount of convective heat loss from the sample, especially when the external heater is on. This is the main reason why the mass loss rate obtained in this apparatus is always lower and the data is much nosier than data from the NIST apparatus. Second, the oxidation factor is also another cause of the noise in the data. In this study, the oxygen level is brought down by diluting the air around the sample by delivering nitrogen to the sample. The oxygen concentration will not reach as low as 0%, as in the NIST gasification apparatus. According to reference [14], a higher oxygen concentration will lead to a faster gasification process. In this case, even though the oxygen concentration is not zero and will speed up the gasification process of PMMA, the convective heat loss is so significant that it further slows down gasification. Eventually, the gasification process is slowed down, while the oxidation remains an influencing factor.

The concentration of this study is then focused on understanding the gasification environment with the "nitrogen frame" design and eliminating the influencing factors listed above to improve the mass loss rate measurement.

2.4 Gasification Environment and Governing Equation

Figure 9 illustrates the gasification experimental environment.

The influencing factors are listed as:

1). The heat flux set from the cone heater, $\dot{Q}_{cone\ heater}$. This heat flux is set before the gasification test is performed. A heat flux gauge is placed at the center of the sample surface level under the cone heater, feeding back to the computer the incident heat flux. The computer will then set different temperature at the cone heater to give different heat flux if the incident heat flux is different from the set value. In this study,

both 50kW/m^2 and 35kW/m^2 are of interest. And the sample surface is 40mm from the cone heater.

2). The convective heat loss. As discussed above, the convective heat loss is large in this case due to the direction in which the nitrogen is delivered. The noise of the mass loss rate measurement is also believed to result from the same reason.

3). The re-radiation. Due to the high surface temperature of the sample during the gasification process, the re-radiation is also an important consideration in the experimental environment. The re-radiation is related to the temperature difference between the sample surface and the ambient air. It is also related to the emissivity coefficient of the surface of the testing materials.

4). The absorption of heat flux by the products of gasification. From the observation of the gasification test, it is clear the gasification products (might be some visible or invisible vapors or particles) are produced and concentrated in between the cone heater and the sample as a result of the way of delivering nitrogen. It is possible that a fraction of χ of radiation from the cone heater is absorbed by these products.

5). The oxidation factor. As reviewed in some previous studies [14], a non-zero oxygen concentration in the gasification test is believed to speed up the gasification process.

Therefore, net heat flux come into the sample is:

$$\dot{q}_{in} = (1 - \chi)\dot{Q}_{cone\ heater} - \varepsilon\sigma(T_{sur}^4 - T_o^4) - h(T_{sur} - T_o) \quad (1)$$

As pointed out in the introduction of this study, one of the biggest advantages of the gasification test is that it is able to give researchers well understood boundary conditions. The flame/auto-ignition of the testing material under the cone heater is able to be removed such that there will not be additional heat flux from the flame, which is the most challenging to quantify in bench-scale fire and material testing. Thus, in the design of the "Nitrogen Frame", all the influencing factors causing uncertainties to the boundary conditions should be well analyzed so that it will be possible to improve the apparatus and simulation.

2.5 The Uniformity of Heat Flux from the Cone Heater

The cone heater in the NIST gasification apparatus and the one in the standard cone calorimeter used in this study are different. Table 2 lists the differences between these two heaters.

<p align="center">Table 2. Different between Cone Heaters in NIST and in this Study</p>

Heater in NIST Apparatus	Heater in this study
300mmm in diameter	160mm in diameter
Three coiled elements	One coiled element
Constant 808°C at heater, different distance from the heater gives different heat flux	Different temperatures at the cone heater gives different heat flux at a certain distance from the heater

As shown above, the heater in the NIST gasification apparatus is supposed to give a more uniform heat flux onto an 80mm by 80mm sample in this study. The uniformity of heat flux in this study is extremely important. On one hand, it ensures that the heat flux profile and the total energy from radiant heat flux during the gasification

test are at the same level as the set heat flux; on the other hand, it enables a one-dimensional heat flux into the sample from the sample surface, which will give a more reliable validation data for the one-dimensional simulation result.

A check for the uniformity of the heat flux at the sample surface is performed. The sample surface was divided into several 20mm by 20mm squares as illustrated in Figure 10. It is assumed that within each 20mm by 20mm measuring squares, the heat flux is uniform. A Schmidt-Boelter heat flux gauge (HFg) in diameter of 7 mm is placed at the center of each measurement square to measure the heat flux at different positions at the sample surface level.
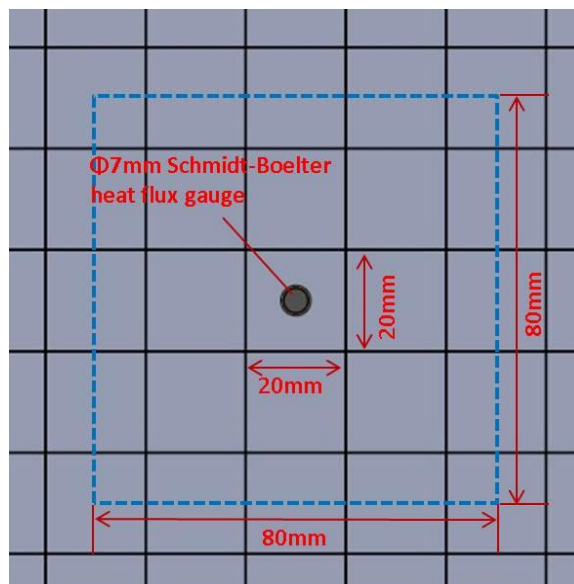
Figure 10. Heat Flux Measurement Areas at the Sample Surface

The 80mm by 80mm sample surface (dashed lined square in Figure 10.) then consists of three kinds of measurement areas. The first one is made up of nine 20mm by 20mm squares in the center; the second kind is the twelve 10mm by 20mm rectangular areas along the four sides of the sample surface; the third kind is the four 10mm by

10mm squares at the four corners of the sample surface. Before the test, the heat flux

at the center of the sample surface is set to be $\dot{H}F_{center}$ (kW/m^2). During the test, the

HFg was placed in the center of the twenty five 20mm by 20mm measurement squares,

then twenty five measurements were taken at different positions along the sample

surface, recorded as HF_1 to HF_{25} (kW/m^2) . The measurements are summarized in

Figure 11.
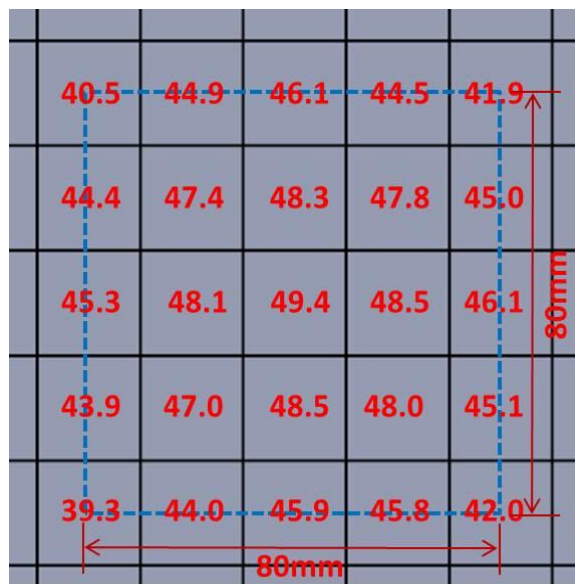
Figure 11. Heat Flux Measurements at Sample Surface with the "Nitrogen Frame"

In this test, $\dot{H}F_{set}$=50.0kW/m^2. As the distance of the measurement point gets farther

from the center point of the sample surface, the heat flux drops significantly. At the

corner of the sample, the heat flux is as low as approximately 40kW/m^2. Figure 12

shows how non-uniform the heat flux distribution is at the sample surface.
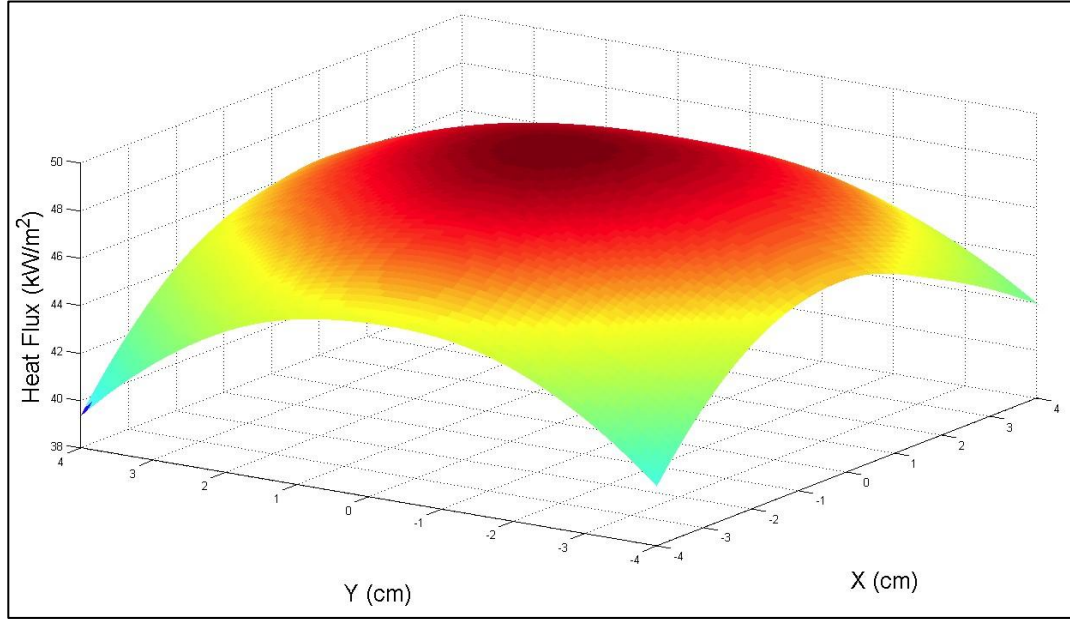
Figure 12. The non-Uniformity of Heat Flux at the Sample Surface

In order to make some corrections account for the uniformity of the heat flux received by the 80mm by 80mm sample during the gasification tests, the uniformity coefficient β_{uni} is introduced in this study. The calculation of this coefficient is:

$$\beta_{uni} = \left. \frac{\frac{\sum_i HF_i * A_i}{A_{sample}}}{HF_{center}} \right. *100\% \quad (2)$$

where HF_i is the measurement taken at different measurement areas as shown in Figure 10. and A_i is the corresponding area of the measurement area. As analyzed above, there are nine areas at the center part of the sample which are 20mm by 20mm, twelve areas along the four sides of the sample which are 20mm by 10mm and four areas at the four corners of the sample which are 10mm by 10mm squares. A_{sample} equals to 80mm by 80mm. HF_{center} equals to 49.4kW/m^2. Finally, the β_{uni} is calculated to be 93%.

With this heat flux uniformity coefficient, a correction is performed in order to give a more accurate heat flux during the gasification tests. For example, if 50kW/m^2 ($\dot{Q}_{cone\ heater}$) is the heat flux under which the gasification test is executed, the HF_{set} should be calculated as:

$$HF_{set} = \dot{Q}_{cone\ heater}\Big/ \beta_{uni} \qquad (4)$$

Since the radiant heat flux is only related to the temperature of the cone heater and the temperature of the sample by the equation of $\dot{q} = \sigma(T^4_{cone\ heater} - T^4_{sample})$, and the distance from the cone heater to the sample surface is set to be 40mm. It could be determined that, the uniformity coefficient with different $\dot{Q}_{cone\ heater}$ is not changed. Thus, HF_{set}=53.8kW/m^2 gives a sample surface averaged $\dot{Q}_{cone\ heater}$ of 50kW/m^2 while HF_{set}=37.6kW/m^2 gives a sample surface averaged $\dot{Q}_{cone\ heater}$ of 35kW/m^2.

2.6 The Convective Heat Loss and Measurement Noise

With the design of this "Nitrogen Frame" installation, the nitrogen is almost flowing out from the orifices on the frame tubes directly onto the surface of the sample. This brings two problems: the convective heat loss and measurement noise. These two situations are able to be improved by adjusting the parameters of the "Nitrogen Frame" settings, namely, the nitrogen flowing angle, α; the nitrogen flow rate coming into the tube frame, FR$_{N2}$; the relative height from the upper edge of the tube frame to the surface of the sample, h. h>0 when the upper edge of the tube frame is above the level of the sample surface level and h<0 when the upper edge of the tube frame is below the

level the sample surface level; and finally, the exhausting flow rate, FR_{ex}. All these parameters are illustrated in Figure 5.

2.6.1 The Measurement Noise

Figure 13 illustrates how much the noise nitrogen flow can bring into the "Nitrogen Frame" gasification system. With the cone heater off and mass balance measurement on, the noise baseline of the mass measurement is recorded either with the nitrogen flow off or on. The comparison shown in Figure 13 can indicate that it's necessary to take efforts to reduce the measurement noise.
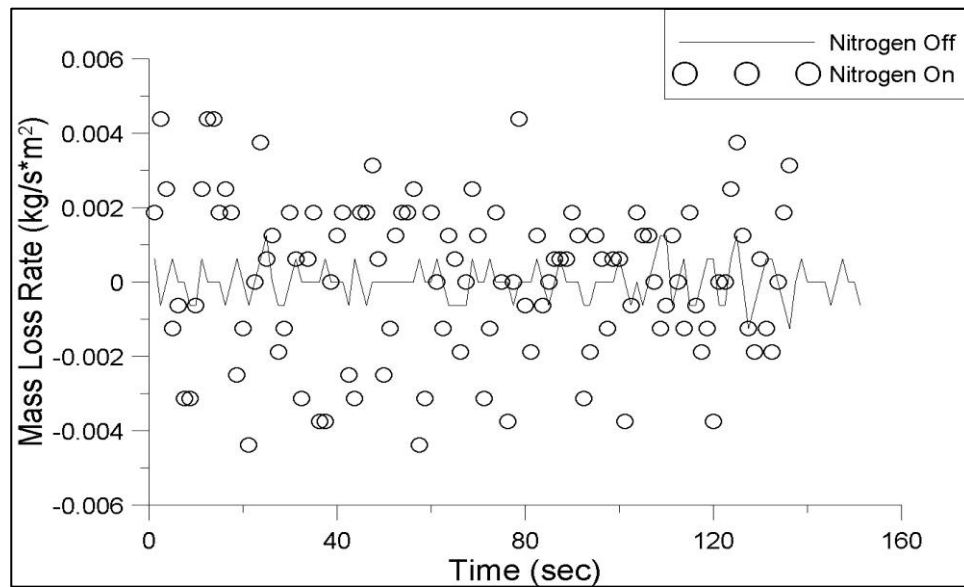
Figure 13. Noise Baseline Comparison (Between Nitrogen on and off)

With nitrogen flow off, the noise recorded is the system noise. The standard deviation of the noise baseline is 0.0005. When the nitrogen flow is turned on, the mass measurement noise recorded is not only system noise but also the nitrogen flow noise. Then the standard deviation of the noise baseline goes up to 0.0021. It is four times as big as the noise with the nitrogen off.

Different combinations of those parameters listed above are tested to determine the optimal setting which minimizes the measurement noise and convective heat loss. In experiments, it is found practically that FR_{N2} should be at least 100SLPM to ensure the auto-ignition to be stopped. FR_{ex} should be at least 24L/s to stop the gaseous decomposition products produced during the tests from being released and potentially harming the investigators. Thus, only the nitrogen flow direction angle α and the relative height of the "Nitrogen Frame" are taken into consideration here. A series of combinations of α and h are tested then and the mass loss rate noise baseline (MLRNB) is recorded. The standard deviations of these measurements are calculated. The combination with the smallest standard deviation is considered the optimal setting.

Table 3. MLRNB Measurements to Determine the Optimal Setting

MLRNB STDEV α \ h	0mm	-10mm	-20mm	-30mm	-40mm	-50mm
45°	0.0026	-	-	-	-	-
60°	0.0022	0.0023	-	-	-	-
75°	**0.0016**	**0.0016**	-	-	-	-
90°	0.0022	0.0021	0.0025	0.0022	0.0031	0.0038

Results are listed in Table 3 below.

By setting α to be 75° and h to be 0mm or -10mm (the upper edge of the frame tube is 10mm lower than the sample surface level), the standard deviation of the mass loss rate noise baseline is minimized with the value of 0.0016.

Thus, the optimal setting of "nitrogen frame" gasification apparatus occurs when FR_{N2} = 100SLPM, FR_{ex} = 24L/s, h = -10mm and α = 75°. With this setting, the "Nitrogen Frame" gasification apparatus gives a significantly improved gasification mass loss rate measurement for PMMA under 50kW/m^2 of external heat flux (HF_{set} = 53.8kW/m^2). It is compared with the original mass loss rate measurement in Figure 14.

It is clear that the MLR profile obtained in this study is improved significantly. The measurement noise is reduced and the average MLR profile is closer to the reference profile obtained by the NIST gasification apparatus.
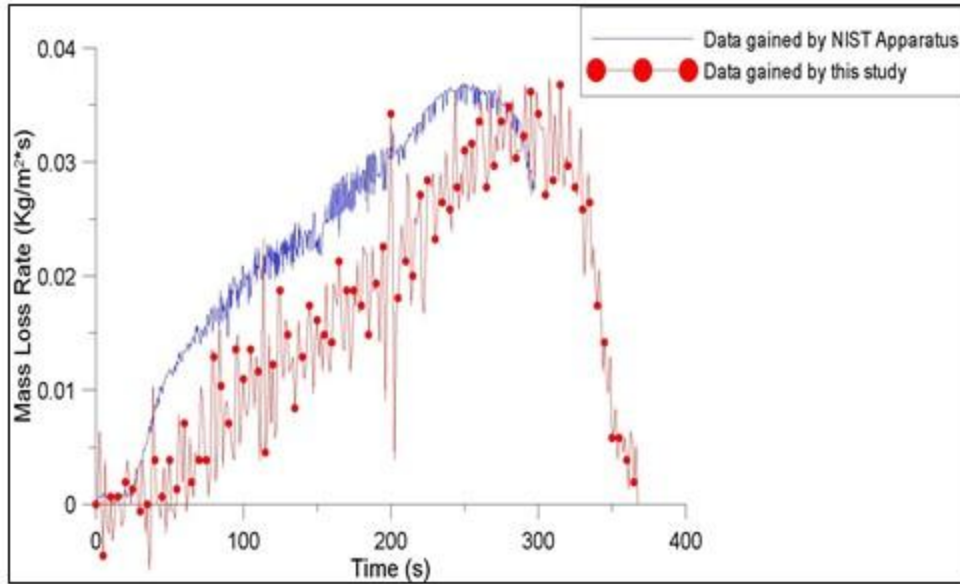
(a)
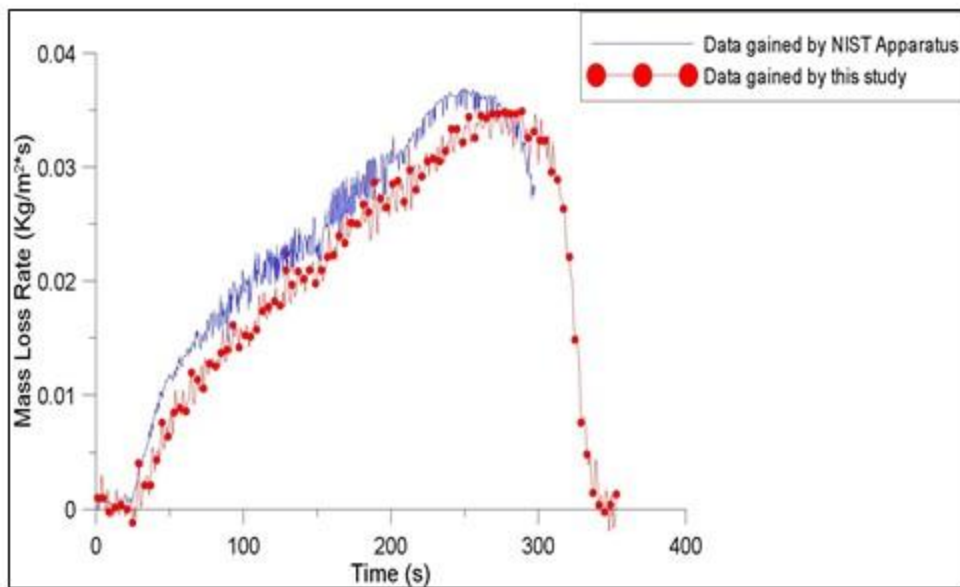
(b)

Figure 14. Comparison between MLR measurement (NIST and "Nitrogen Frame" Apparatus) of PMMA under 50kW/m^2 before (a) and after (b) the Optimal Setting

2.6.2 The Convective Heat Loss

Even though the mass loss rate measurement has been improved, the MLR profile by this study is still lower than the reference profile by NIST apparatus. It is hypothesized that the convective heat loss is the principal reason. Therefore, this section will give an approach to quantify the convective heat loss.

Based on the convective heat transfer theories, to calculate the convective coefficient, various information needs to be analyzed and quantified. As shown in Figure 9, the information includes parameters such as: the horizontal velocity of the nitrogen flow; the temperature of the nitrogen flow, the temperature of the sample surface, etc. To quantify the horizontal velocity of the nitrogen flow, all factors such as the direction of the nitrogen flow, the nitrogen flow rate and the relative position of the frame tube to the sample need to considered. To quantify the temperature of the nitrogen flow, thermocouple is not a good choice since the cone heater is giving constant radiant heat flux during the test. The temperature of the sample surface is also not easy to be quantified not only because of the cone heater, but also because of the difficulties in measuring the surface temperature. Besides the surface of the sample is being gasified, increasing the measurement difficulty even more. Last but not least, the nitrogen flow over the sample during the gasification process is likely to be unstable, which creates further uncertainty in quantifying the convective coefficient by hand calculations.

A fire testing simulation model called Thermo-Kinetic Model of Burning (ThermaKin) is used in this study to help quantify the convective heat loss during gasification. ThermaKin is a one-dimensional model developed by Dr. Stanislav I.

Stoliarov solving the non-steady energy and mass conservation equations accounting for chemical reactions described by a reaction mechanism. The sample material is defined in Thermakin geometrically as a series of layers with specified thicknesses and chemically as material components defined by specific physical and chemical properties. If the properties of testing materials such like the density, heat capacity, thermal conductivity, mass transport coefficient, emissivity, and absorption coefficient are defined and input into the ThermaKin model, the heat and mass transfer progress will be able to be well simulated. This model has been validated on different charring or non-charring materials [19, 20].

To evaluate the convective coefficient in the "Nitrogen Frame" gasification environment, the sample is replaced by a piece of 80mm by 80mm copper (3mm thick) sheet under the cone heater. The surface of the copper is painted black, giving a known emissivity coefficient (0.94) of the sample surface. The surface of the copper is 40mm from the cone heater. The "Nitrogen Frame" is set to the optimal setting (FR_{N2} = 100SLPM, FR_{ex} = 24L/s, h = -10mm and α = 75°). The cone heater is set to 50kW/m^2. Then, four thermocouples are inserted into the center layer of the copper sheet to measure the temperature of the copper. The configuration is illustrated in Figure 15. A normal gasification test using the "Nitrogen Frame" but with the copper sheet sample is performed while the temperature change of the copper is being measured.

The governing equation describing the gasification environment with a copper sample is shown in Equation (3).

$$\dot{q}_{in} = \dot{Q}_{cone\ heater} - \varepsilon\sigma(T_{sur}^4 - T_o^4) - h(T_{sur} - T_o) \quad (3)$$
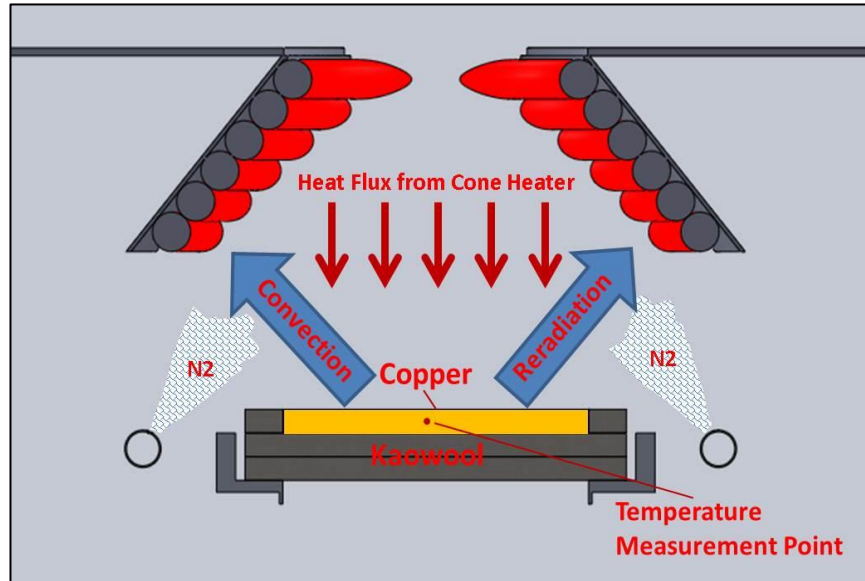
However, in this experiment, the governing equation becomes much simpler. The $\dot{Q}_{cone\ heater}$ has been analyzed and is more uniform with the uniformity coefficient β_{uni} corrections. The re-radiation part, $\varepsilon\sigma(T_{sur}^4 - T_o^4)$, can be well defined in the ThermaKin simulation. The absorption and oxidation factors are removed since the copper cannot be gasified. Thus, the only unknown parameter in the equation (1) is the convective heat loss, $h(T_{sur} - T_o)$.

ThermaKin is used to simulate this special gasification test on copper. Since there will be no chemical reactions in this test, only the physical properties of copper and kaowool board need to be inputted into the ThermaKin input file. In the boundary condition file, the radiant heat flux is well defined while the convective coefficient is not known yet. In order to solve for this variable, a preliminary guess is input into ThermaKin. The temperature profile of the copper sheet is simulated by ThermaKin and compared with the experimental data. Once the experimental data fits the simulated data, the h value is proved to be valid. This process is illustrated in Figure 16.
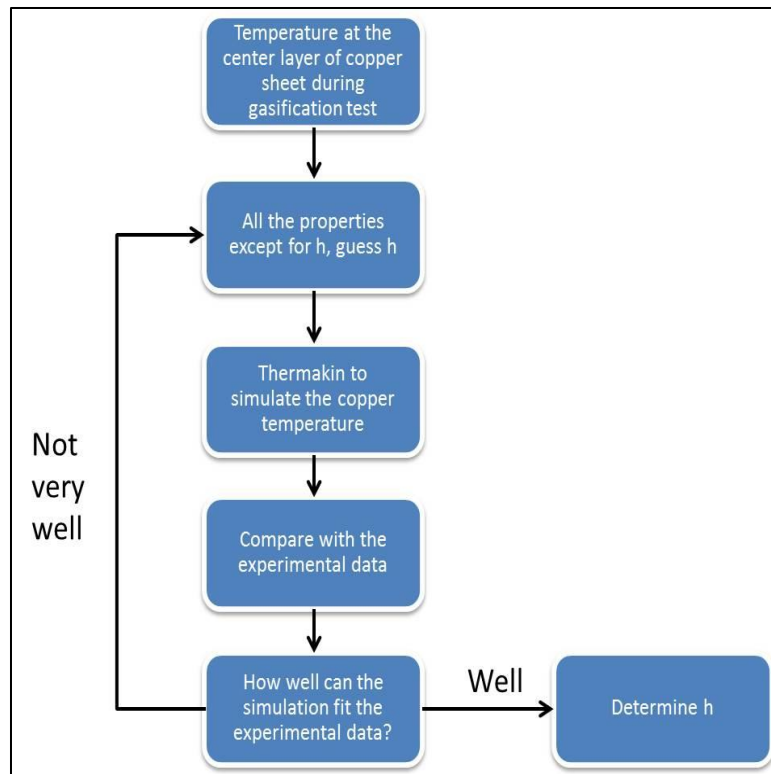
Figure 16. Procedure of Determining Convective Coefficient, h

Another important influencing factor in this test is the resistance of the black coating on the copper sheet surface to the high temperature. During this test, the steady-state temperature of the copper sheet will reach as high as 600 °C. However, the black coating can only resist as high as 200 °C according to the tech specs of the black coating used here. After 200 °C, the black coating on the copper sheet will start to degrade and the boundary condition will change. If the boundary condition of the experiment and the one of the simulation are not the same, the comparison becomes pointless. Thus, even if a temperature profile shown in Figure 17 could be obtained, the only valid comparison should be on the curve where the temperature is below 200 °C
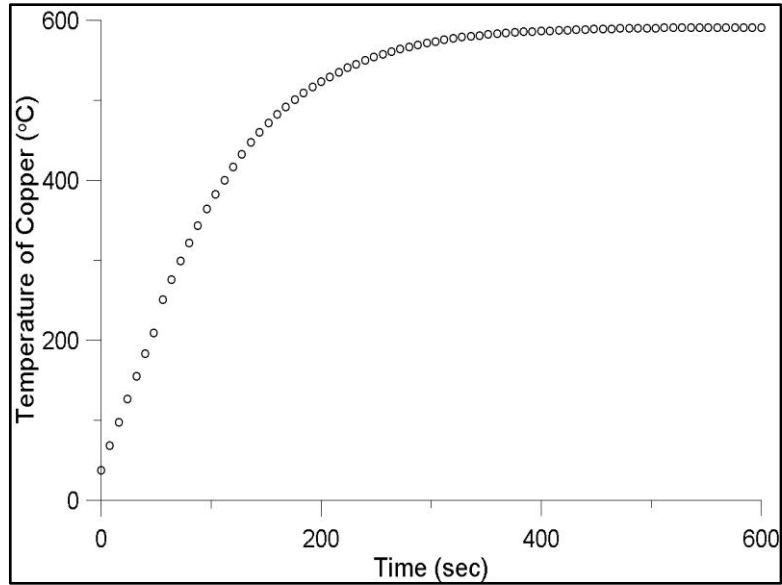
Figure 17. Copper Temperature Profile in Gasification Environment

Figure 18 below shows the comparison between the experimental measurement and the simulated results. When a convective coefficient of h=50W/m^2*K is input into the ThermaKin simulation file, the simulated results appear to fit the experimental data
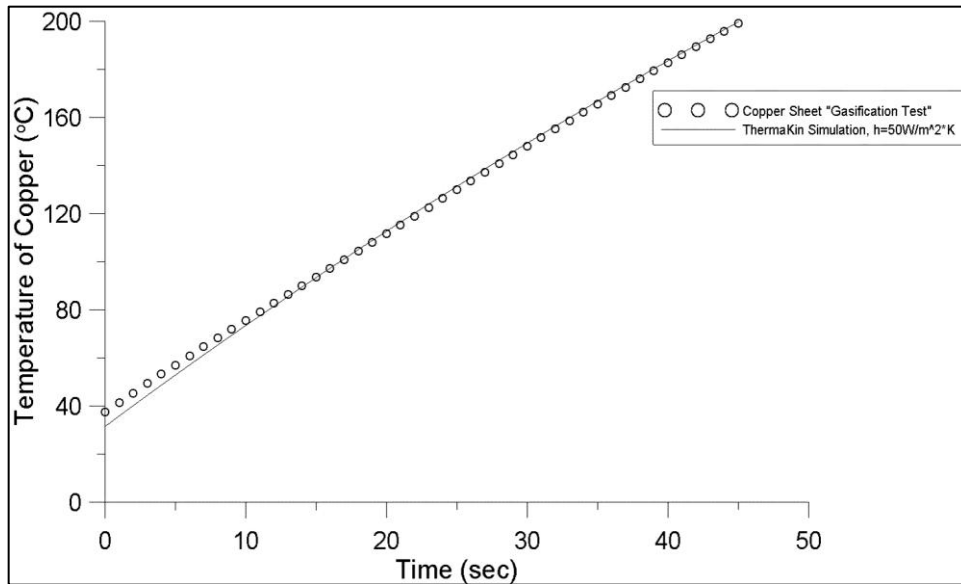
Figure 18. Copper Temperature Comparison, Experiment VS. Simulation

well. Thus, it is concluded that the convective coefficient under the "Nitrogen Frame" gasification environment is 50W/m^2*K.

2.7 Absorption Factor

Another factor is the absorption of the radiant heat flux in between the cone heater and the sample during the gasification tests. From the observation, it is evident that the polymer being gasified produces a lot of "white smoke" that is concentrated in between the cone heater and the sample by the nitrogen flow coming out from the orifices on the frame. This white smoke most likely consists of some vapors or gaseous polymer products. It is opaque and it stays there for 60% of the time during the test. If this smoke absorbs a portion of the radiant heat flux from the heater, then the heat flux received by the sample during the gasification would be below the set value. It is very important to understand whether this white smoke absorbs a certain amount of the heat flux. If this is true, it is necessary to determine how much of the heat flux is being absorbed.

A test to determine the absorption factor is designed. A hole 7 mm in diameter is drilled at the center point of a piece of 80 mm by 80 mm PMMA sample. Then the HFg (also 7 mm in diameter) is placed inside the hole. The HFg is then inserted from the bottom of the sample holder and the top of the HFg is placed 5 mm above the surface of the sample. This configuration is illustrated in Figure 19.

For the first test, a normal gasification test is executed and the heat flux is recorded. Then in the second test, the PMMA sample is replaced by a piece of 80 mm by 80 mm Kaowool PM board. The insulation is able to withstand high temperatures, and

therefore it does not produce any smoke like a polymer sample produces. The difference between these two tests is the smoke produced by the PMMA sample during gasification. If the heat flux reading in the Kaowool test is lower than that in the PMMA gasification test, it proves that the smoke produced by the PMMA absorbs some heat from the cone heater. The difference between these two tests will be the amount of heat flux absorbed.
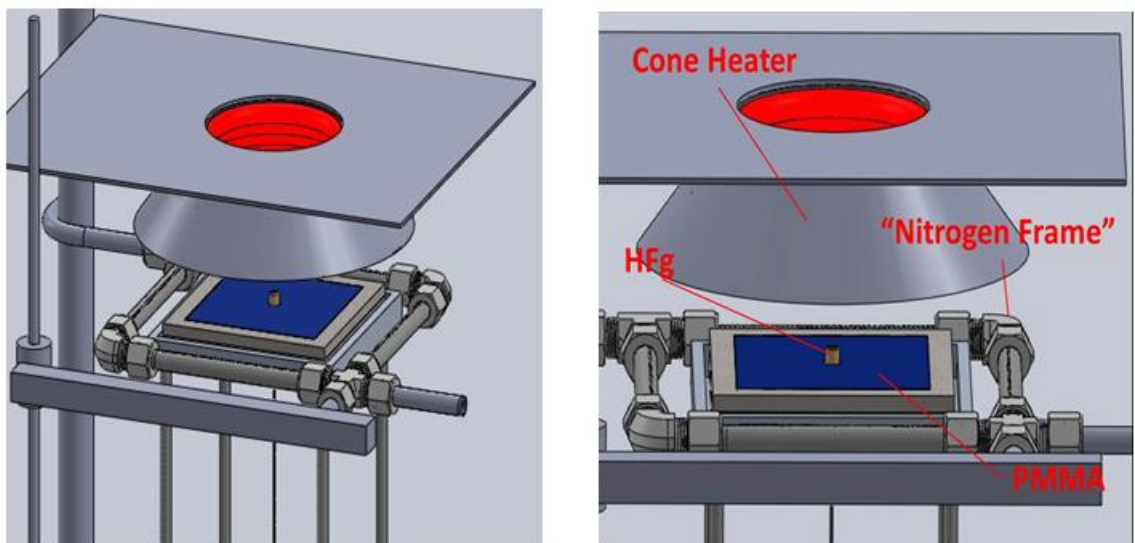
Figure 19. Configuration of the Measurement of Absorption Factor

The heat flux measurements from these two tests are shown and compared in Figure 20.
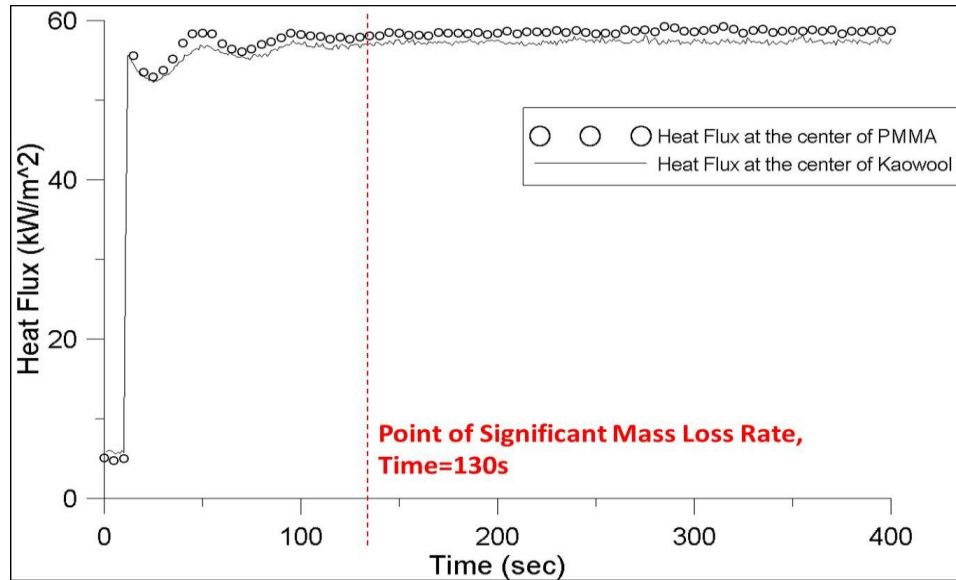
Figure 20. Heat Flux Measurement at the center of PMMA and Kaowool

The smoke produced from the gasification of PMMA starts at 130 seconds from the start of the test. If the smoke produced by the gasification of PMMA does absorb or block some radiant heat flux from the cone heater, the heat flux measurement in the PMMA test should be decreasing when the smoke is produced and accumulates between the cone heater and the PMMA sample. In Figure 20, it is evident that the heat flux profile takes some time to reach the steady reading. This is the nature of a heat flux measurement with this kind of gauge. 130 seconds from the start of the test, the heat flux profile of the PMMA test and that of the kaowool test follow the same development trend. The fact that the heat flux measurement of the PMMA test does not have the trend of decreasing is clear evidence indicating that the smoke produced by PMMA does not absorb or block the radiant heat flux from the heater. Thus, the absorption part in the governing equation, Equation (1), can be removed. The updated governing equation is:

$$\dot{q}_{in} = \dot{Q}_{cone\ heater} - \varepsilon\sigma(T_{sur}^4 - T_o^4) - h(T_{sur} - T_o) - oxidation \quad (5)$$

2.8 Oxidation Factor

To measure the oxygen concentration at the sample, a probe is connected to the sample pump of the standard cone calorimeter. The gas about 2 mm above the sample surface is collected by the probe and delivered into the gas analyzer of the cone calorimeter through sample pump. The gas analyzer then gives the reading of the volumetric concentration of the sample gas at the sample surface.

Based on previous studies [14], the oxidation factor does have some effect on the PMMA gasification process. However, this influence is very small if we take a look at the results observed in reference [14] (shown in Figure 21.). The oxidation factor for PMMA is also observed to have little effect. Although the local oxygen concentration is measured to be around 15% by volume, the mass loss rate profiles obtained from the
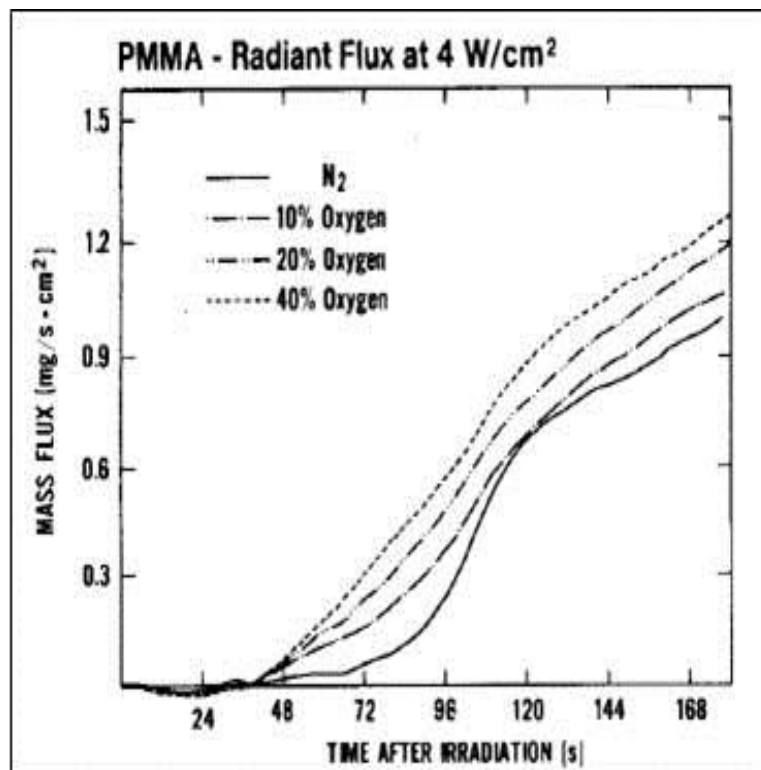
Figure 21. Oxidation Factor on PMMA per reference [14]

"Nitrogen Frame" apparatus are still very close to the reference profile obtained by the

NIST apparatus (where the oxygen concentration is 0%). It is therefore concluded that

PMMA is not very sensitive to oxygen, especially when compared to the Polypropylene

(PP) case which will be discussed later.

2.8.1 The Gasification Test on PP by "Nitrogen Frame" Apparatus

Since satisfactory measurement results are obtained for PMMA with the

"Nitrogen Frame" apparatus, it was used on another commonly used polymer -

Polypropylene (PP). Several gasification tests are executed for PP under an external heat

flux of 50kW/m^2 with the optimal setting of "Nitrogen Frame" used for PMMA.

However, the auto-ignition is not able to be stopped in any of these tests. The PP

gasification tests are then executed under an external heat flux of 35kW/m^2, which is

the other heat flux of interest in this study. No auto-ignition occurs, and the gasification

mass loss rate profile is obtained and compared in Figure 22.
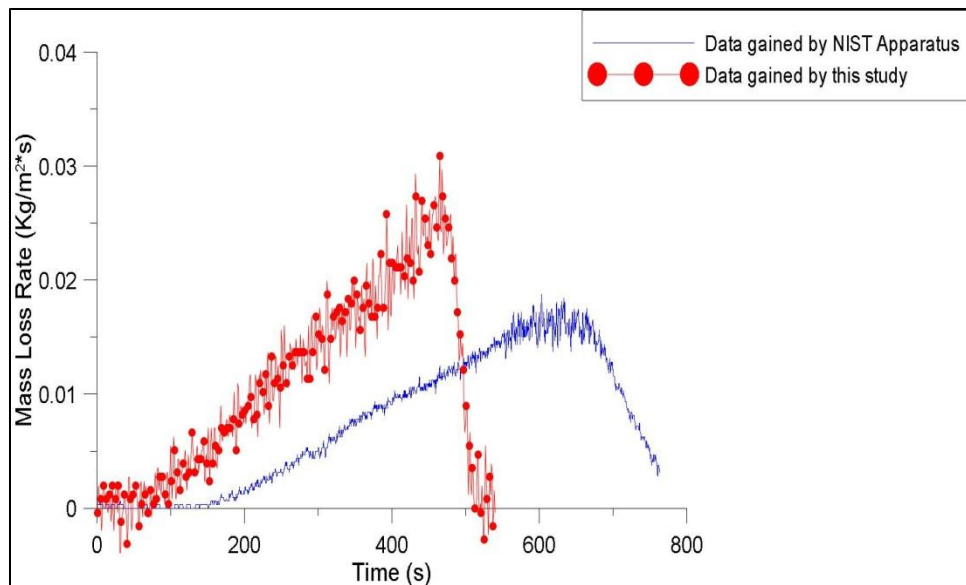
Figure 22. Comparison between MLR measurement (NIST and "Nitrogen Frame" Apparatus) of PP under 35 kW/m^2

The gasification mass loss rate profile obtained in this study for PP is significantly faster than the one obtained by the NIST apparatus under the same heat flux. In reference [14], there was no study on the influence of oxygen on PP. If we compare the chemical structure and molecular formula of PMMA and those of PP in Figure 23, the question why PP is more sensitive to oxygen can be answered.

From the chemical structures of PMMA and PP, it a reasonable guess that PP is more sensitive to oxygen in high temperature environment because that in PMMA, there are oxygen atoms, but in PP, there are no oxygen atom. To prove this hypothesis, some additional tests are conducted.

2.8.2 The 1% Oxygen Enclosed Chamber Gasification Test

One of the cone calorimeters in the lab has a chamber securing the testing area, which has the capability of being used to perform enclosed chamber cone calorimeter tests. Some PP gasification tests are executed in this enclosed chamber cone calorimeter, where the oxygen concentration can be reduced to approximately 1%. If the oxidation factor is the main cause of the differences between the data sets seen in
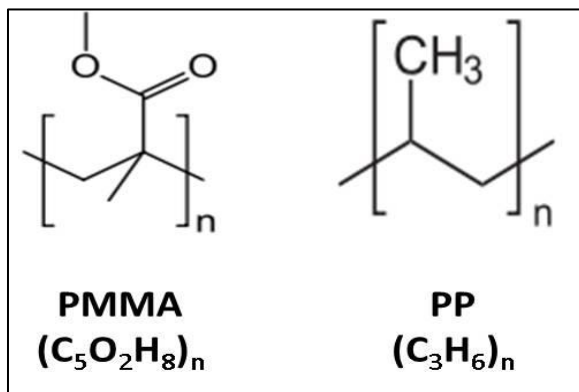
Figure 23. Comparison between Chemical Structures of PMMA and PP

Figure 23, the gasification mass loss rate profile obtained here should be much lower than the one obtained in the "Nitrogen Frame" gasification apparatus and very close to the one obtained in the NIST gasification apparatus. Figure 24 shows some pictures of this enclosed chamber low oxygen gasification tests.
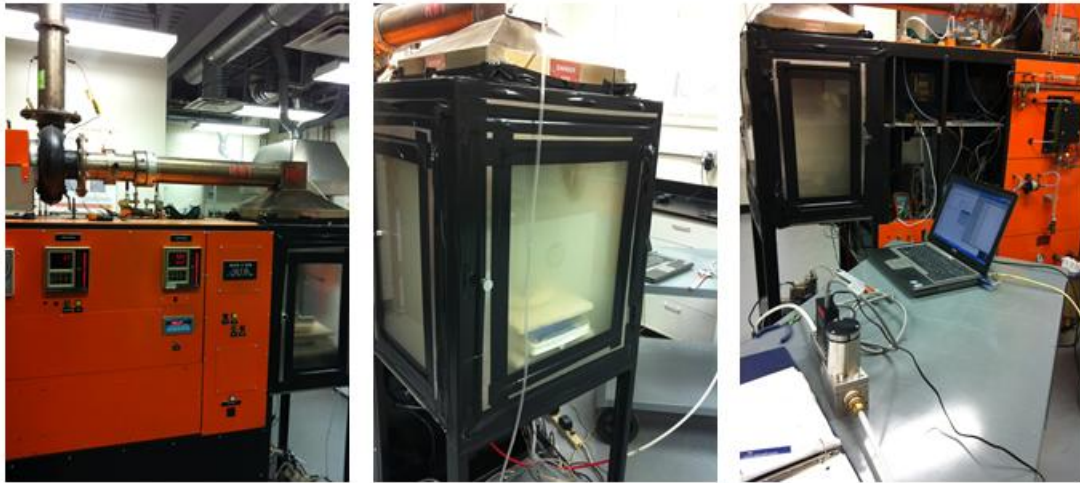
Figure 24. Pictures Showing the Enclosed Chamber Gasification Tests

The whole chamber is sealed with heat resistant tape to make sure that there is no exchange of air in between inside and outside of the chamber. A laptop is used to collect the mass loss rate data during the gasification test. High purity nitrogen purges the chamber of air from the bottom of the chamber at a rate of 500SLMP. The oxygen concentration at the sample is measured to be 1% by volume. The mass loss rate measured in this test is compared with both the data obtained in NIST apparatus and the data obtained in "Nitrogen Frame" apparatus in Figure 25.

The results show the influence of oxygen on the gasification process of PP. When the oxygen volumetric concentration is reduced from 15% (in "Nitrogen Frame" tests) to 1% (enclosed chamber gasification tests), the gasification mass loss rate of PP decreases significantly.
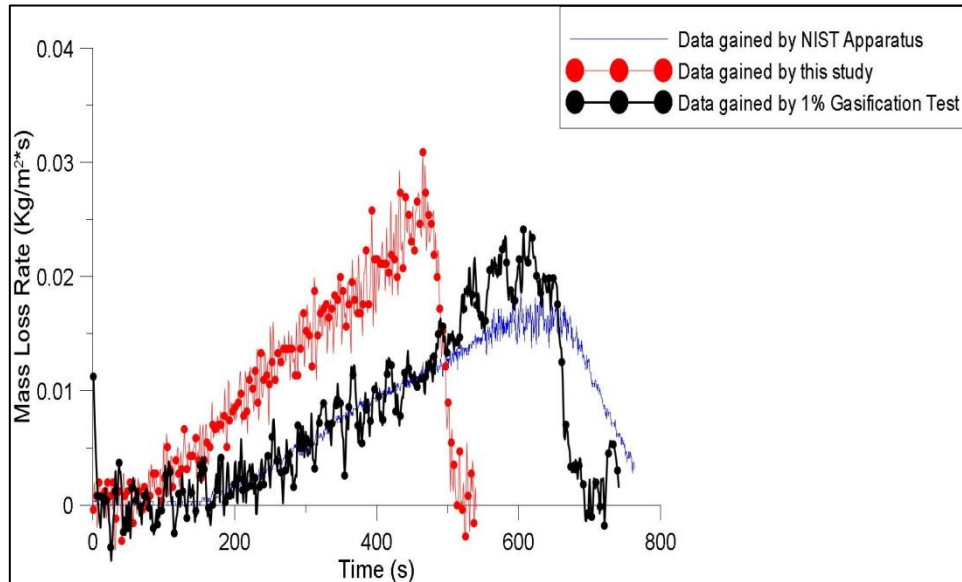
Figure 25. Comparison between gasification MLR measurements (NIST, "Nitrogen Frame" Apparatus and 1% oxygen enclosed chamber) of PP under 35kW/m^2

2.9 Discussion of Results of "Nitrogen Frame" Apparatus

As analyzed in this section, the first version of the design of gasification apparatus - "Nitrogen Frame" is successful for the PMMA sample. The auto-ignition or flaming is successfully stopped; the optimal setting of this apparatus is determined after many tests, the governing equations and boundary conditions for this apparatus are well understood; the uniformity coefficient of the cone heater is determined to help improve the radiant heat flux; and the convective coefficient can to be quantified with the ThermaKin simulations. This apparatus is capable of giving good enough gasification mass loss rate measurements of PMMA.

However, oxidation is a problem in this design. As analyzed in the final part of this chapter, it can be concluded that the oxygen concentration achieved by the "Nitrogen Frame" apparatus (15% by volume) is not satisfactory. It may be good enough for the gasification test on some polymers which are not sensitive to oxygen, such like PMMA. But, for polymers like PP, the gasification mass loss rate measurement will always be higher than expected, and therefore invalid. Furthermore, the oxidation factor is hard to quantify in the fire testing simulations models.

This first version of design appears not able to solve the gasification problem for different kinds of polymers. However, it cannot be denied that a lot of valuable knowledge has been gained from the "Nitrogen Frame" testing. It is evident from these tests that the oxygen concentration must be reduced further to obtain reasonable results.

More efforts are taken to design a second version of the gasification apparatus in this study: the "Controlled Atmosphere Pyrolysis Apparatus", or CAPA.

3. Gasification Apparatus Design - "Controlled Atmosphere Pyrolysis Apparatus"

3.1 Modification of the "Nitrogen Frame"

As analyzed in the last chapter, the "Nitrogen Frame" Apparatus must be abandoned because the oxygen concentration that results from using this apparatus cannot be reduced to an effective level. The oxidation factor, although not very significant in the PMMA case, has a significant influence on the PP case. Additional efforts are taken to reduce the local oxygen concentration by creating an improved version of the gasification apparatus.

From examining the testing done using the "Nitrogen Frame", it is believed that air is introduced to the sample from the four sides as well as from the tubes below the frame, as illustrated in Figure 26.
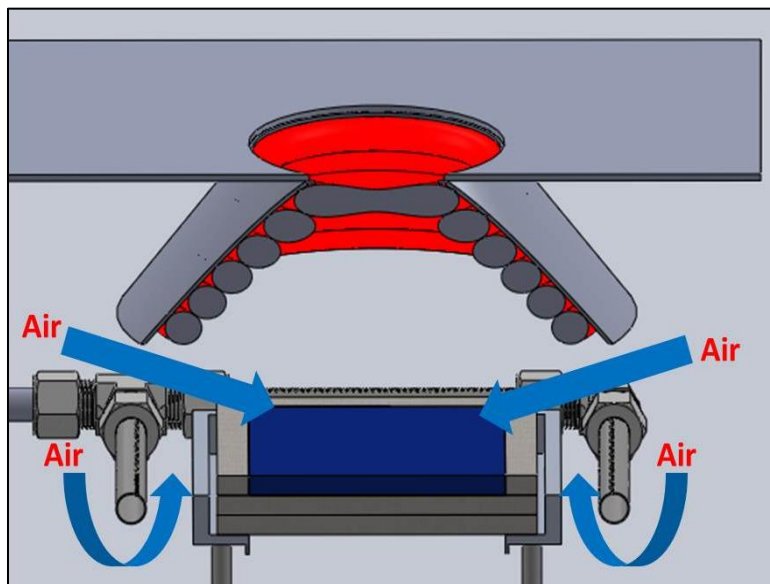
Figure 26. The Paths of Air in "Nitrogen Frame" Gasification Case

Some quick modifications are implemented on the "Nitrogen Frame" to reduce the oxygen concentration around the sample by blocking those paths as is shown in

Figure 26. Some pieces of aluminum sheets are shaped and mounted around the "Nitrogen Frame" and the local oxygen concentration is measured. The configuration of this test is shown in Figure 27.
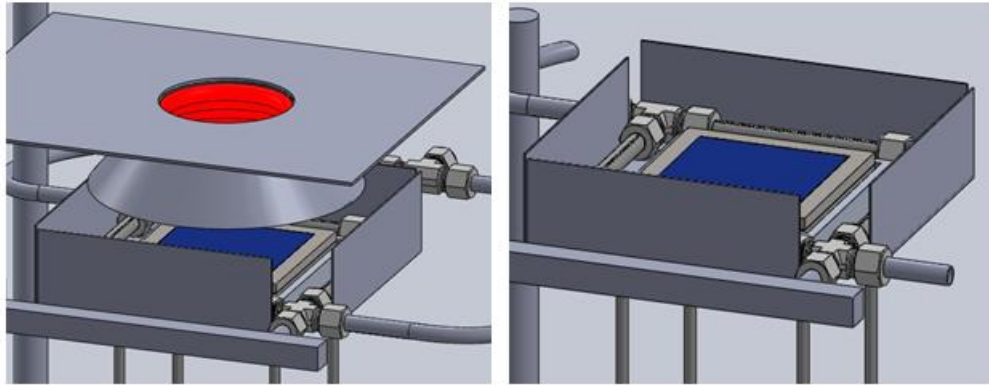
Figure 27. Quick checks of Local O2 Concentration after Air Paths Blocked

With the blocks in place, the local oxygen concentration around the sample is reduced to 8% from 15%. Even though the blockages are not very well engineered at this point, the oxygen concentration at the sample is still reduced by a significant amount. Therefore, to reduce the local oxygen concentration, the space around the sample should be more carefully enclosed. The open atmosphere is to be kept in this new design, the re-radiation from the gasification apparatus is to be kept at a minimum level. It is therefore preferred that the air paths are blocked by nitrogen flow instead of metal walls. With these ideas and experiences, a new version of gasification apparatus is designed and constructed.

3.2 The Controlled Atmosphere Pyrolysis Apparatus - "CAPA"

This new version of gasification apparatus design is called the "Controlled Atmosphere Pyrolysis Apparatus" - "CAPA". Figure 28 shows a picture of the constructed apparatus.

Figure 28. Picture of "Controlled Atmosphere Pyrolysis Apparatus"

The detailed design of CAPA is illustrated in Figure 29. In this design, high purity nitrogen is divided into four paths and then it is introduced to in between the inner wall and outer wall of the opened box from each inlet at the bottom of the four sides. Hundreds of glass beads are packed right above the inlet of nitrogen to make sure that the nitrogen is uniformly distributed and moving at a similar velocity upwards towards the sample. The upper edge of the inner wall of the apparatus is 10mm below the surface of the sample, while the upper edge of the outer wall is 10mm above the

surface of the sample. This reduces the re-radiation from the apparatus to the sample

blocks the air paths. The sample, kaowool insulation and the sample holder is placed in

the interior volume at the center of the apparatus. The horizontal opening area of the

interior volume is 120mm by 120mm, which is a little bigger than the size of the surface

area of the sample holder (115mm by 115mm). This ensures that the air paths from the

bottom of the sample and sample holder are blocked as much as possible; furthermore,

it leaves the sample and sample holder clear from the inner wall of the CAPA so that

valid mass loss rate measurements are guaranteed.
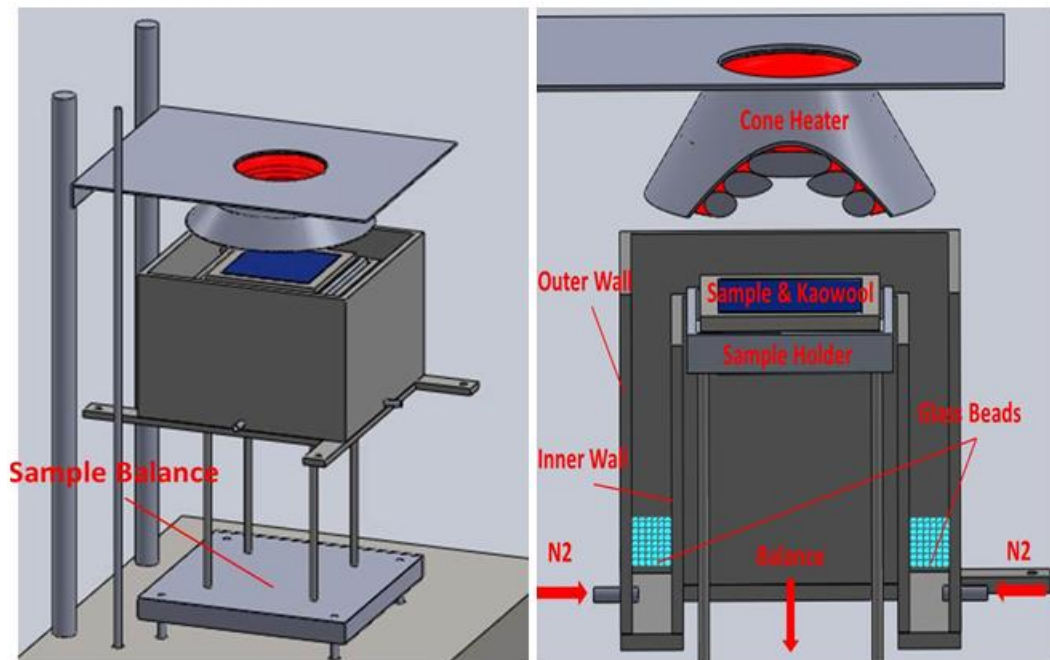
Figure 29. Detailed Design of "Controlled Atmosphere Pyrolysis Apparatus"

The well-mixed nitrogen flows upward from in between the inner wall and outer

wall of the apparatus. The nitrogen performs two functions: dilute the oxygen around

the testing materials under the heater and function as a "wall of nitrogen", stopping air

from the four sides from coming into the apparatus. The local volumetric oxygen concentration around the sample is significantly reduced by this new design.

3.3 The Oxygen Concentration Measurements in the CAPA Environment

3.3.1 With the Cone Heater Off

The testing material is replaced by a piece of Kaowool board (100mm by 100mm) for this test. An oxygen probe is placed about 3mm above the surface of the Kaowool to measure the oxygen concentration. Nine points over the sample are tested to check the uniformity of the oxygen concentration. When 200SLPM of high purity nitrogen is pumped in to this system, the results are summarized in Figure 30.

Figure 30. Oxygen Concentration at the Sample Surface with CAPA, Cone Heater is Off

It is encouraging to see that the oxygen concentration at the sample, even with the cone heater off, is reduced a lot. The oxygen concentration with the "Nitrogen Frame" apparatus is as high as 15%, but with the CAPA, the average oxygen concentration is around 2.4%. Furthermore, the oxygen is very uniformly distributed

over the surface of the sample. With this oxygen concentration, it is expected that the oxidation factor will be significantly reduced in PP gasification test.

3.3.2 With the Cone Heater On

Several gasification tests for PP are conducted in CAPA testing environment with FR_{N2} = 200SLPM, however, the auto-ignition is not stopped in any of the test. The same test as the one in section 3.3.1 is then performed, but the cone heater is turned on to be 50kW/m^2. The oxygen concentration in this case is still very uniform, but the average value jumps to as high as around 12.5%.

The difference between the average oxygen concentration between these two tests (2.4% with the cone heater off while 12.5% with the heater set to be 50kW/m^2) indicates the fact that the heat flux from the heater has a significant effect on the oxygen concentration in CAPA testing environment. When the whole system is under the cone heater, the temperature of the gas around the sample will increase significantly. Bigger buoyancy effect causes additional flow from outside to the sample. As a result, the oxygen concentration around the sample increases dramatically.

As in the "Nitrogen Frame", the air is probably coming in from the bottom of the equipment since the sides are sealed off and have a steady supply of nitrogen to push out incoming air. This pattern is illustrated in Figure 31.
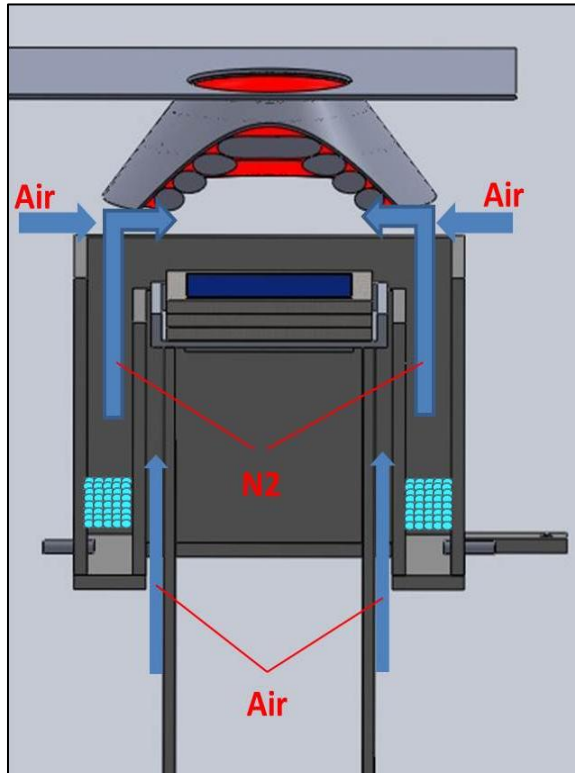
Figure 31. Paths of Air in CAPA Environment

Some modifications of the CAPA are made in order to reduce the oxygen concentration at the sample surface.

3.4 Modification of CAPA for Lower Oxygen Concentration

A piece of aluminum plate used to block the air from the bottom of the apparatus. Four holes with diameters of 10 mm, which is a little bigger than the diameter of the legs of the sample holder, are drilled into the plate. The four legs of the sample holder are able to fit through the holes in the aluminum shield, as shown in Figure 32(a). The aluminum plate is attached to the bottom of the CAPA.
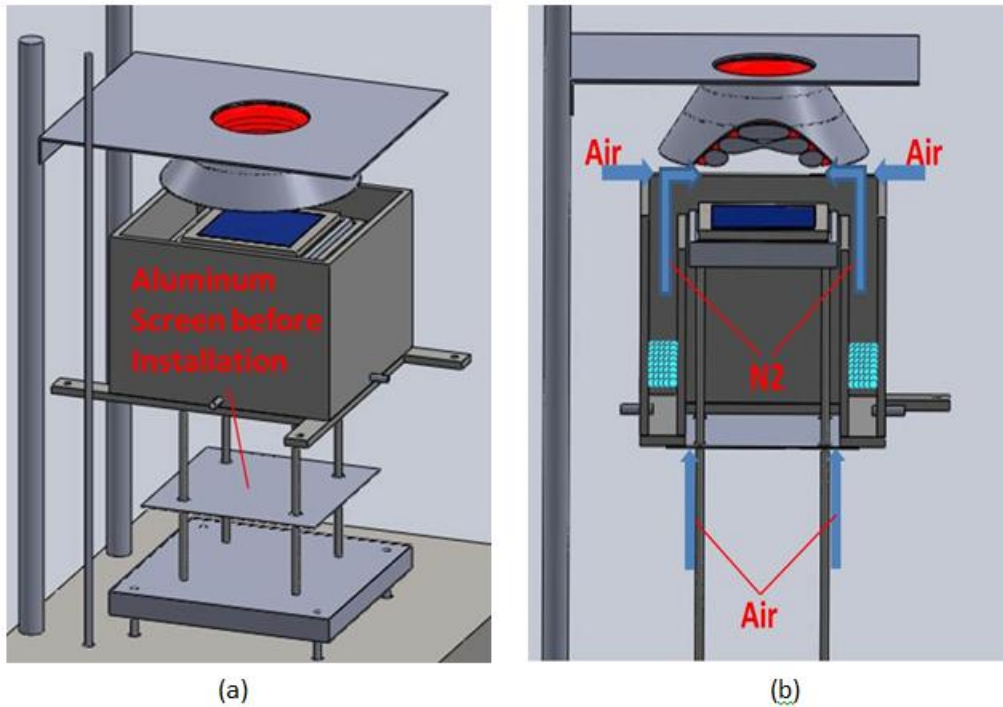
Figure 32. (a).Installation of the Aluminum Screen to the Bottom of CAPA. (b).Gas Flows in the CAPA Environment after the Installation of Aluminum Screen.

The air and nitrogen flows in the CAPA environment are affected by the aluminum shield as shown in Figure 32 (b). The air from the bottom is blocked from coming to the sample even if the heater is on.

The same oxygen concentration measurement is executed after the CAPA is modified, Figure 33 shows the results with the cone heater set to be 50kW/m^2 and FR_{N2} of 200SLPM. The average oxygen concentration is 3.1%, which is much lower than the 12.5% before the aluminum screen at the bottom is installed. If a higher flow rate of high purity nitrogen is introduced into the system, the oxygen concentration is even reduced further. With cone heater set to be 50kW/m^2 and FR_{N2} of 250SLPM, the oxygen concentration measurement is as shown in Figure 34.

Figure 33. Oxygen Concentration in CAPA Environment, with Cone Heater at 50 kW/m^2 and 200SLPM of N2

The average oxygen concentration is calculated to be 2.1%, which is as low as the oxygen concentration measured with the cone heater off in section 3.3.1.

Figure 34. Oxygen Concentration in CAPA Environment, with Cone Heater at 50 kW/m^2 and 250SLPM of N2

If the nitrogen flow introduced into the system was increased to an even higher flow rate, it is expected that the oxygen concentration at the sample could be reduced to nearly 0%.

In this study, since the cost of nitrogen is a factor, the nitrogen flow is set to be 200SLPM. An oxygen concentration of around 3% is expected to be low enough for the PP tests.

3.5 The Uniformity of Heat Flux from the Cone Heater

As discussed earlier, the cone heater used in this study is not able to give a uniform enough heat flux at the sample surface. In the "Nitrogen Frame" case, the uniformity coefficient β_{uni} is measured and calculated to be 93%. In CAPA case, since the design is very different from the "Nitrogen Frame", the β_{uni} is expected to change. Thus, a heat flux uniformity test should also be done on this new design.

Same as the one executed on the "Nitrogen Frame" case, the sample surface of 80mm by 80mm is divided into 20mm by 20mm squares. It is assumed that the heat flux measured in each measuring squares is uniform with in the 20mm by 20mm area. There are three kinds of measuring areas over the sample surface. The first one is the nine 20mm by 20mm squares at the center part; the second one is the twelve 20mm by 10mm areas along the edges of the sample surface; the third one is the four 10mm by 10mm squares in the four corners of the sample surface. The definition of the uniformity coefficient β_{uni} is:

$$\beta_{uni} = \frac{\frac{\sum_i HF_i * A_i}{A_{sample}}}{HF_{center}} * 100\% \quad (6)$$

Due to the design of the CAPA, the sample should be taken out from the system when the heat flux is measured at the level of sample surface (40mm from the cone

heater). To locate the Schmidt-Boelter heat flux gauge (HFg) in the interior volume, several metal wires are mounted along the inner wall of the apparatus, leaving twenty-five 20mm by 20mm openings for the measurement. The configuration is illustrated in Figure 35.
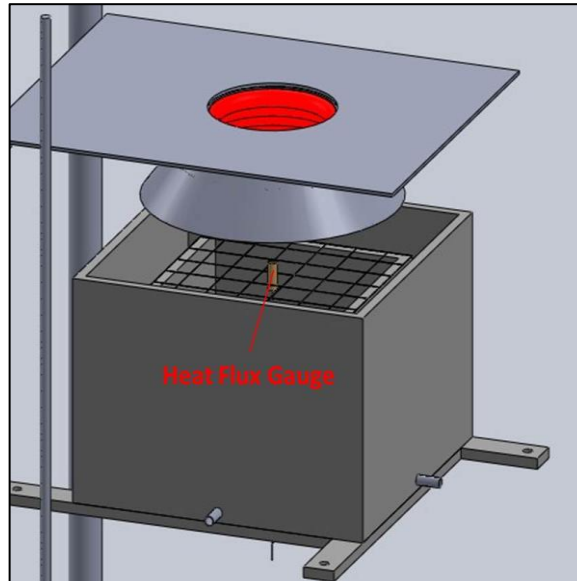
Figure 35. The Heat Flux Uniformity Measurement on "CAPA"

The HFg is placed at the center of the each measuring area. The surface of the HFg is 10mm above the upper edge of the inner wall of the apparatus, ensuring that the surface of the HFg is at the same level as the surface of sample in gasification tests. The measurements are taken with FR_{N2} of 200SLPM and the HF_{set} set to 50kW/m^2. The results are shown in Figure 36.

By these measurements, the β_{uni} is calculated to be equal to 94.9% for CAPA gasification environment. The heat flux distribution is more uniform over the sample surface in the CAPA apparatus than with the "Nitrogen Frame" apparatus.
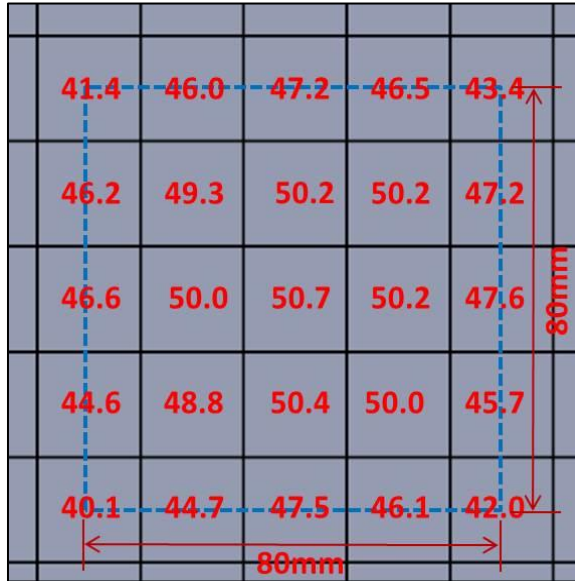
Figure 36. Heat Flux measurements at the sample surface with CAPA

Finally, in the CAPA gasification test, HF_{set}=52.7kW/m^2 gives a sample surface averaged $\dot{Q}_{cone\ heater}$ of 50kW/m^2 while HF_{set}=36.9kW/m^2 gives a sample surface averaged $\dot{Q}_{cone\ heater}$ of 35kW/m^2.

Since the upper edge of the outer wall of the CAPA is 10mm higher than the surface of the sample, the re-radiation from the CAPA to the sample is also a factor to concern. In another test, the CAPA is exposed to the cone heater for 10 minutes. Then the heat flux distribution is measured again when the temperature of the CAPA is at least around 500 °C. If the re-radiation affects the sample surface, these measurements should be bigger than the first heat flux measurements. However, the result turns out to be close to the first measurement, drawing a conclusion that the re-radiation from the CAPA to the sample surface is negligible.

3.6 Mass Loss Rate Comparison.

Some gasification tests of PolyPropylene (PP) are conducted in the CAPA environment described above. The FR_{N2} is set to be 200SLPM, the cone heater gives a radiant heat flux of 50kW/m^2 (HF_{set}=52.7kW/m^2). The auto-ignition of PP is successfully stopped in every test and reproducible gasification mass loss rate measurements are obtained. The comparison of the averaged data obtained in CAPA and in NIST gasification apparatus is shown in Figure 37.
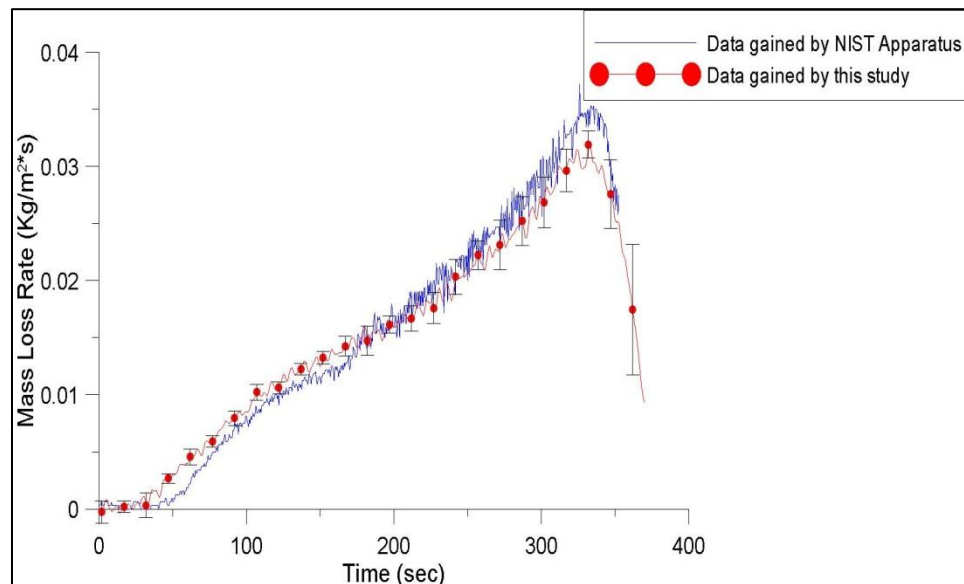
Figure 37. Comparison between MLR measurement (NIST and "CAPA") of PP under 50 kW/m^2

First, the ignition of PP under 50kW/m^2 heat flux is successfully stopped for the first time in this study. In the "Nitrogen Frame" study, the PP is always being auto-ignited under 50kW/m^2, thus on the profile of PP under 35kW/m^2 is obtained. Second, as shown in Figure 37, these two gasification mass loss rate profiles are very close to each other. The gasification process starts at the same time in both cases, and the peak values of the MLR are also very close. However, one point needs to be noted in the mass loss rate obtained by the CAPA. In the early part (time ≤ 200sec) of the CAPA

measurements, the mass loss rate is a little faster than the NIST data; while in the later part (time ≥ 200 s) the mass loss rate is a little slower than NIST data. This indicates that the convective heat loss is also a big influencing factor in the CAPA case. In the first half of the test, the surface temperature of the sample is not as high as in the later part of the process. This results in convective heat loss, which is proportional to the temperature difference between the temperature of the sample surface and ambient air. This heat loss is therefore smaller in the earlier part of the test and increases as the temperature of the surface increases. This is the cause of the trend seen in the data in Figure 37.

3.7 Gasification Environment and Governing Equation

The governing equation for the CAPA gasification environment is very similar to that in the "Nitrogen Frame" gasification environment:

$$\dot{q}_{in} = (1 - \chi)\dot{Q}_{cone\ heater} - \varepsilon\sigma(T_{sur}^4 - T_o^4) - h(T_{sur} - T_o) - oxidation \quad (7)$$

However, there are key differences between the Equation (1) and Equation (7) as listed below:

1). The heat flux from the cone heater. It is different since the uniformity coefficient β_{uni} in the CAPA gasification environment is different from the one in "Nitrogen Frame" case, as discussed in section 3.5. The heat flux with the CAPA is more uniformly distributed at the level of the sample surface (the β_{uni} is lower). And the re-radiation from the CAPA to the sample surface is negligible.

2). The convective heat loss and measurement noise. As analyzed with the "Nitrogen Frame", the convective heat loss and the noise in the data have a large effect

because of the design of the apparatus. These factors are largely reduced by determining the optimal setting of the frame tube. The convective coefficient is estimated to be around 50 W/m^2*K. In the CAPA gasification environment, the convective heat loss as well as the noise of the measurement is much smaller than that in the "Nitrogen Frame" apparatus. The mass loss rate profile is much closer to the reference data from NIST and the data points show less variability.

3). The re-radiation from the sample to the ambient environment can be well simulated by ThermaKin, as in the "Nitrogen Frame" gasification governing equation. This will be discussed later.

4). The absorption factor. Because how the products of gasification concentrate between the cone heater and sample is related to the material itself, only PMMA and PP are of interest in this study. Based on the results in section 3.8, the absorption factor of PMMA and PP are negligible. Therefore, the absorption in Equation (7) can be removed.

5). The oxidation factor. The reduction of the oxygen concentration is the main reason that the "Nitrogen Frame" apparatus was improved upon. The local oxygen concentration at the sample surface is reduced from 15% with the "Nitrogen Frame" to 3% using the CAPA. Base on the mass loss rate profile obtained for PP under 50kW/m^2, the oxidation factor is reduced by a significant amount, thus negligible.

Therefore, the governing equation for the CAPA gasification environment should be modified as:

$$\dot{q}_{in} = \dot{Q}_{cone\ heater} - \varepsilon\sigma(T_{sur}^4 - T_o^4) - h(T_{sur} - T_o) \quad (8)$$

3.8 The Convective Heat Loss in CAPA.

To quantify the convective heat loss from the sample surface to the ambient atmosphere in the gasification environment of the CAPA, the same approach described in section 3.6 is also used here. This approach involves using the ThermaKin model to simulate the middle layer temperature of a piece of copper sheet in the gasification environment. Everything in this experiment is the same as the gasification test for polymer materials, but the only difference is that the polymer is replaced by a piece of copper sheet as illustrated in Figure 38.
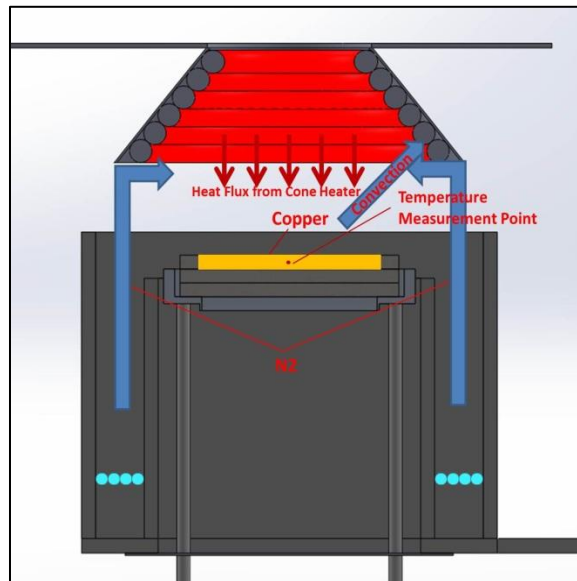
Figure 38. Measurement of Temp. of Copper Sheet to Determine the Convective Coefficient in CAPA

The temperature at the middle layer of the copper sheet is not only measured in the gasification tests, but also simulated by the ThermaKin model. In the ThermaKin simulations, different values for the convective coefficient are used. Then the simulated results and the experimental measurements are compared. The value of the convective coefficient used in ThermaKin is modified until the temperature profiles from the

simulation and the data match up. This value is then taken as the convective coefficient. This procedure is illustrated in Figure 16.

Also, as explained in the section 2.6, since the black coating used on the surface of the copper sheet in this test is only able to survive a temperature of as high as 200°C, he valid comparison between the experimental temperature measurement and the simulated temperature profile should be made below this maximum temperature.

Several different values of convective coefficient are used in the ThermaKin simulations. When the coefficient equals to 15 W/m^2*K, the experimental data and simulated data are of good agreement, the result is shown in Figure 39.

The gasification apparatus in this study has been significantly improved since the convective coefficient is reduced from 50 W/m^2*K to 15 W/m^2*K. Without such a big convective heat loss as estimated in the "Nitrogen Frame", the gasification process will be much more reliable. 15 W/m^2*K should be very close to the convective coefficient
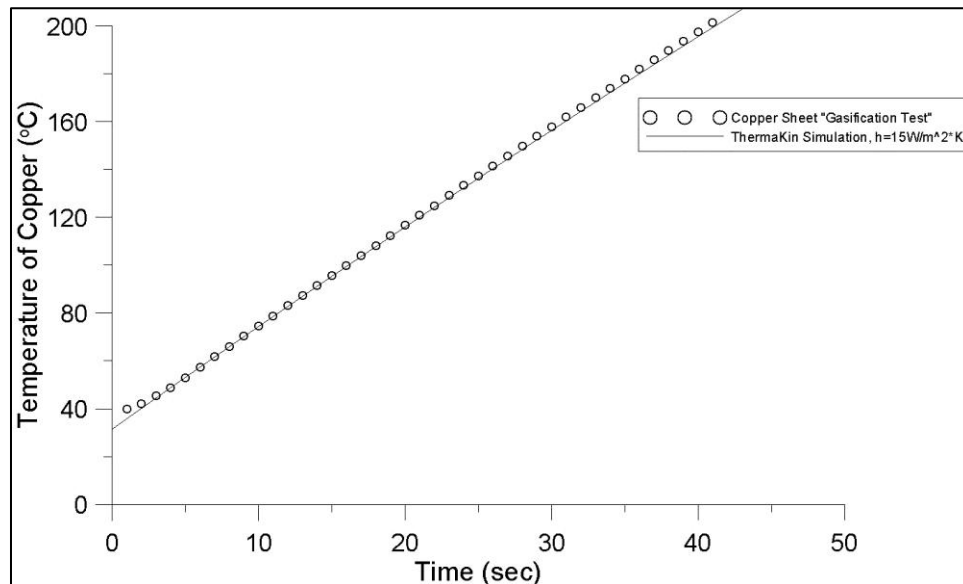
Figure 39. Copper Temperature Comparison in CAPA

in the NIST apparatus.

3. 9 Final Gasification Mass Loss Rate Profiles

At this point, the final version of the gasification apparatus - CAPA, has been successfully designed. The oxygen concentration, as well as the convective heat loss, has been largely reduced to a level where both factors have minor impacts on the gasification processes of both PMMA and PP samples. Under two heat fluxes of interest, 35 kW/m^2 and 50 kW/m^2, reproducible gasification mass loss rate profiles on PP and PMMA samples are obtained with CAPA.

However, the PP sample under 35kW/m^2 is a special case. With 200SLPM of nitrogen introduced in the CAPA (giving 3.1% of local oxygen concentration at the sample), the mass loss rate data is obtained as is shown in Figure 40.

Figure 40. Comparison between MLR measurement (NIST and "CAPA") of PP under 35 kW/m^2, 200 SLPM of Nitrogen

It can be seen that this mass loss rate is higher than the reference data. It is likely to be caused by two reasons, 1). 3.1% of oxygen concentration might be still too

high for the PP sample. The oxidation factor, as analyzed in section 2, may increase the gasification rate of PP significantly. 2). The spectrum of radiation received by the sample in the CAPA apparatus is different from that in the NIST apparatus. Th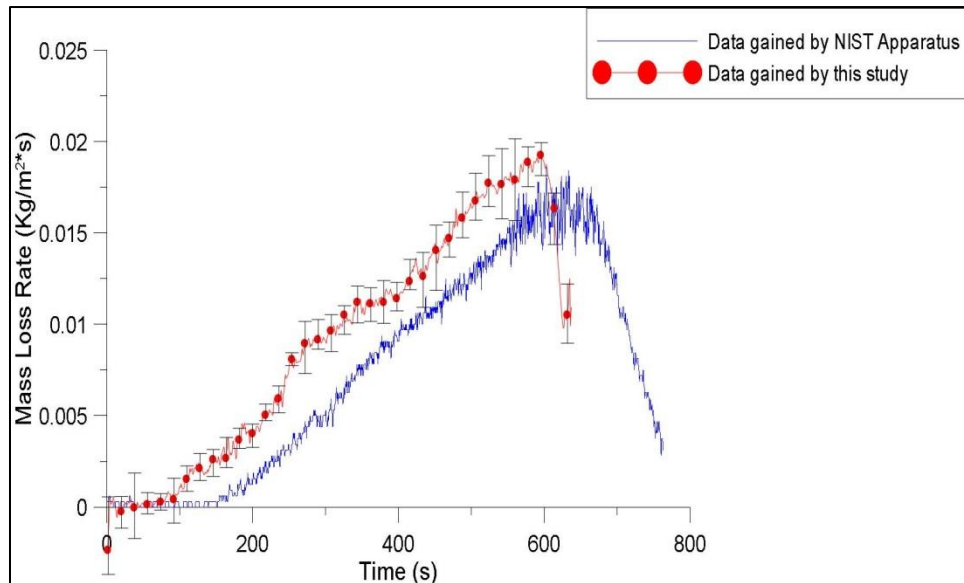e temperature of cone heater in NIST apparatus is 808°C, but that of the cone heater used in this study is at 650°C when it emits 35kW/m^2 of radiant heat flux. This different may result in different depth into which the sample absorbs radiant heat flux. It is likely that this depth is deeper in the CAPA gasification than that in the NIST apparatus. This can partially explain why the mass loss rate difference between the data of this study and the reference data obtained by NIST apparatus under 35kW/m^2 is larger than that under 50kW/m^2. This analysis is also found reasonable in the PMMA tests.

The nitrogen flow is then increased to 250SLPM for the gasification test of PP under 35kW/m^2. This nitrogen flow gives 2.1% of oxygen concentration at the sample surface. The gasification mass loss rate profile is found to be much closer to the NIST reference data than that in the 200SLPM test. Finally, the MLR profiles for PMMA and PP are compared with the reference data from NIST gasification apparatus and shown in Figure 41.
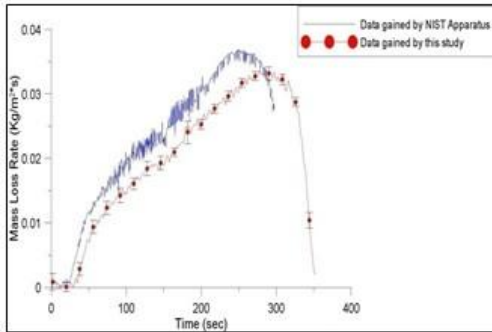
PMMA under 50kW/m^2
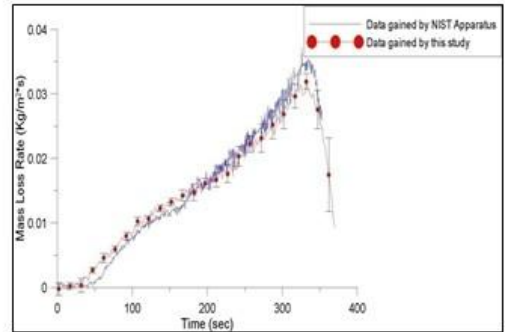
PP under 50kW/m^2
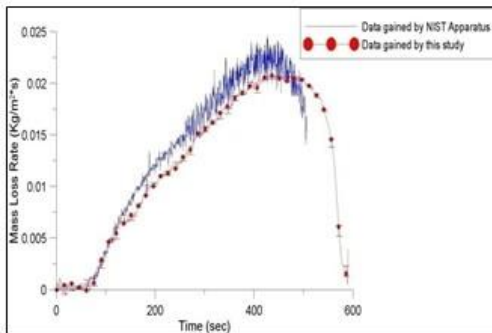
PMMA under 35kW/m^2
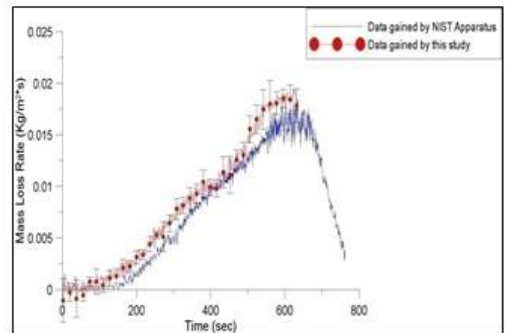
PP under 35kW/m^2

Figure 41. Final Gasification Mass Loss Rate Profiles for PMMA and PP

4. Measurement of Thermal Conductivity (k) and Verification of ThermaKin Simulation

4.1 Introduction to the Thermal Conductivity Measurement

Another objective, as described earlier in this study, is to provide a method to estimate the thermal conductivity of a polymer.

The theoretical background of thermal conductivity is:

$$\dot{q}''_{in} = -k\frac{dT}{dx} \qquad (9)$$

The most classical way of measuring the thermal conductivity is to measure the temperature gradient in the direction of x in Equation (9) when a heat flux is given in direction of x as well. This measurement requires well-engineered equipment which will ensure that, first, the heat flux in to the material is one-dimensional; second, the measurement of the temperature is sufficiently precise. This equipment is usually expensive.

In this study, a new methodology for the measurement of the thermal conductivity is introduced. Similar to the method for determining the convective coefficient, this method also relies on a combination of experimental work and the simulation by ThermaKin.

The main difference is that, in the convective coefficient test, the middle-layer temperature of the copper sheet is measured in the gasification environment and simulated by ThermaKin; but in this section, the back surface temperature of tested polymers being gasified is measured and simulated to determine value of k. The back

surface temperature is chosen because the top layer or any layer in the middle gradually disappears during the gasification processe., This leads to impossibility of measuring the temperatures there. The back surface of the gasified material always stays at the same position of the sample, so that the temperature is possible to be accurately measured. More importantly, since all the boundary layer conditions at the top surface are well defined, the temperature at the top surface is not hard to be accurately simulated. However, for the back surface, everything is unknown. To make the analysis more complete and thorough, the back surface is a better choice. Last but not least, the temperature at the back surface is essentially determined by thermal conductivity, giving another advantage of estimating the thermal conductivity.

The ThermaKin model is also used to simulate the back surface temperature of a testing material when being gasified. To do this, the ThermaKin input file needs all kinds of properties for the testing materials, including: density, ρ; emissivity, ε; absorption coefficient, K_s; heat of reaction, ΔH_r; heat capacity, C_p; activation energy, E; pre-exponential coefficient A, and finally, the thermal conductivity, k. The values of ρ, ε and K_s are either measured or got from literatures; the values of ΔH_r, C_p, E, A are measured by a parallel study on Thermogravimetric analysis (TGA) and Differential Scanning Calorimetry (DSC). After all the properties except for the exact value of k are known, a ThermaKin simulation is used to simulate the back temperature of a testing material with an estimated k. The simulated and the experimental back surface temperature profiles are compared to each other then. If these two profiles can match up quite well,

the corresponding estimated k value is regarded as the thermal conductivity of the testing material. This whole process is illustrated in Figure 42.

The challenges stem from two aspects. The first one is on the experimental work. Researchers have been debating on the measurement of the surface temperature by thermocouples for a long time. In this study, since it is the back surface temperature of the testing material thermocouples are measuring during gasification tests, it is difficult and complicated to get the accurate measurement.
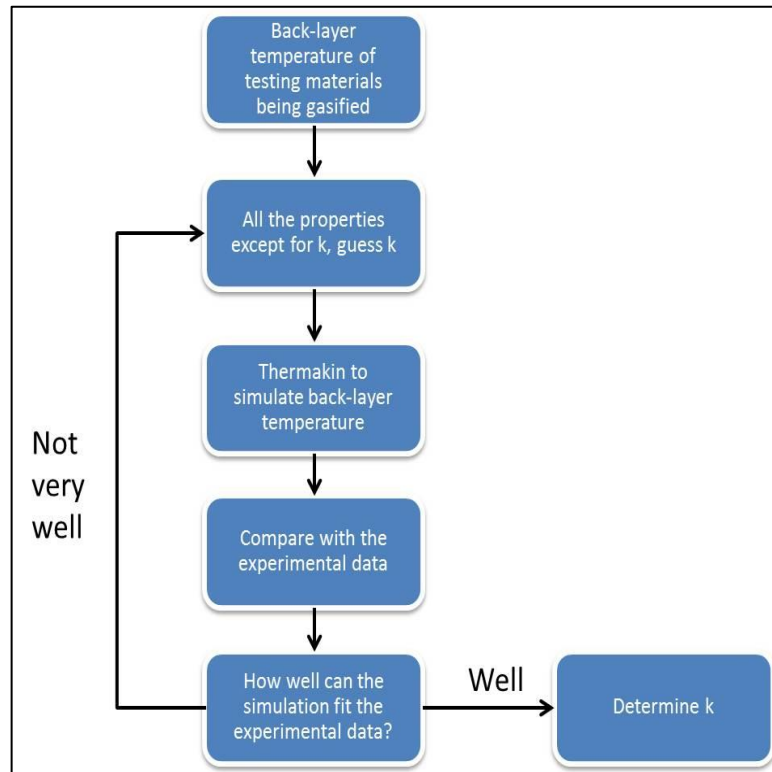
Figure 42. Process of Determining Thermal Conductivity, k

The second challenge is that, the ThermaKin simulation needs not only thermal conductivity but also all other physical and chemical properties of the testing materials. Whether the other properties used in the simulation are sufficiently accurate is also of concern and could have large impact on the final simulation results. Most of the

uncertainties may come from the values of the absorption coefficient and the convective coefficient in the simulation input files, which will be discussed in the later part of this chapter.

The structure of the ThermaKin simulations of the back temperature as well as the gasification mass loss rate is shown in Figure 43.
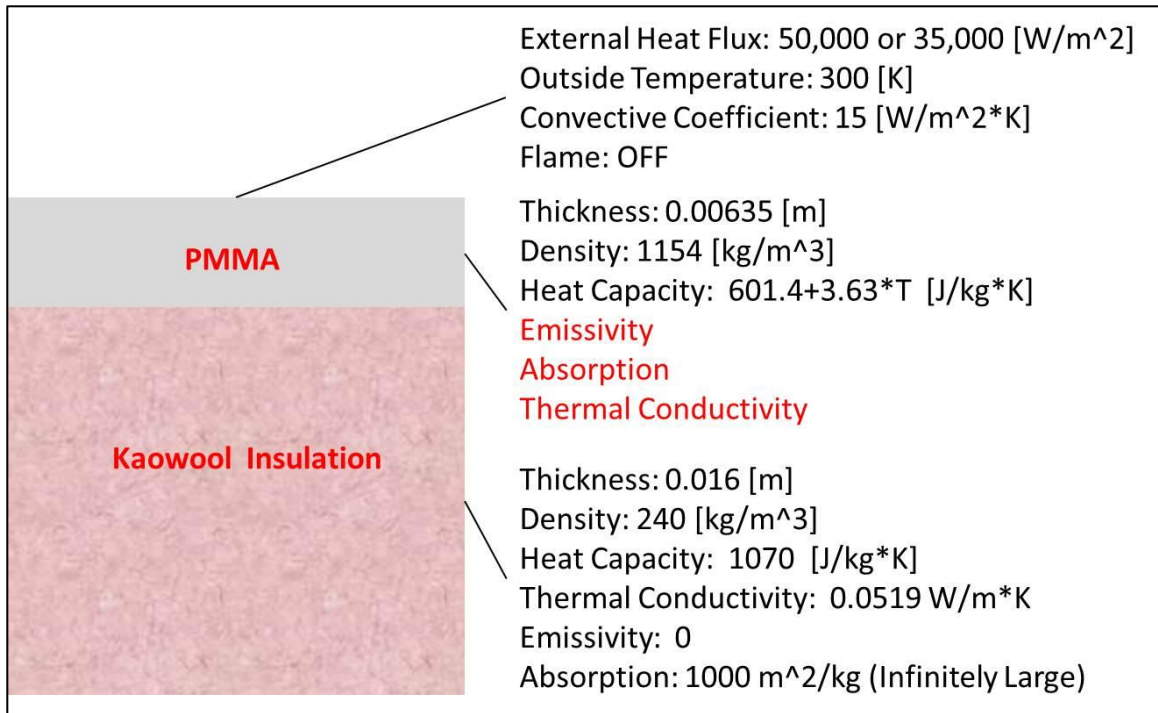
Figure 43. Structure of ThermaKin Simulation

4.2 PMMA Back surface Temperature Measurement

A thermocouple is used to measure the temperature at the back surface of a PMMA sample while it's being gasified in CAPA environment. The thermocouple is 0.25mm in diameter, grounded, of type K and with Inconel 600 sheath. Thermocouples of this diameter are the smallest sheathed thermocouple available. The small diameter and grounded junction of the thermocouple ensures fast response of temperature measurement. Another advantage of the size of the thermocouple is that it does not lift the sample to reduce the distance from the sample to the cone heater. The heat flux received by the sample is still well defined.

The thermocouple is cemented by OMEGABOND® CC High Temperature Cement onto the bottom of the aluminum foil wrapped around the PMMA sample. The cemented point (measuring point) is located at the center of the back surface as illustrated in Figure 44 (a).

(a)   (b)   (c)
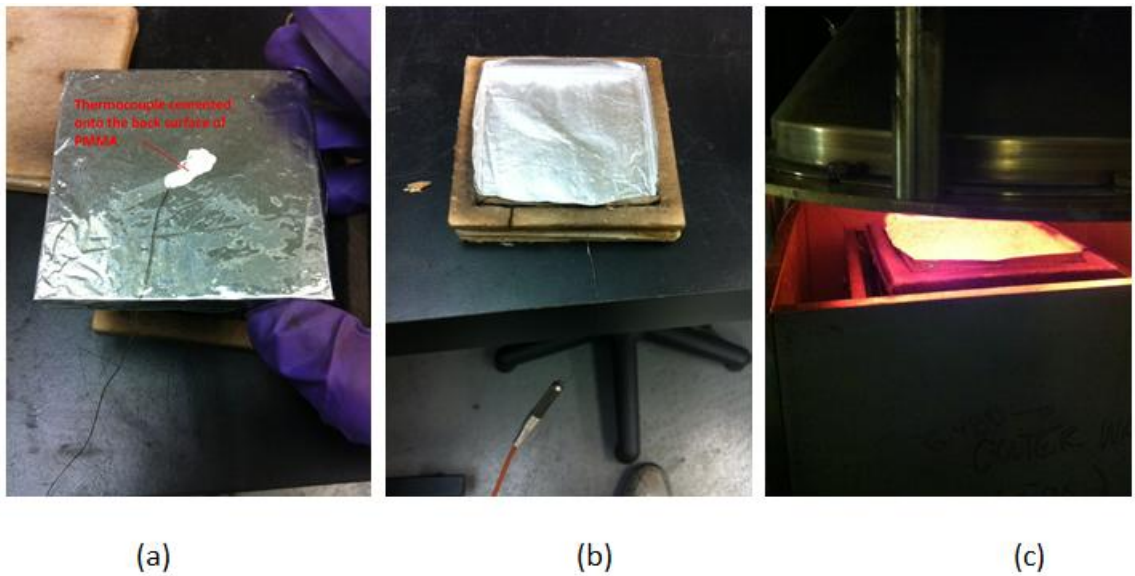
Figure 44. Back surface Temperature Measurement of PMMA

OMEGABOND® CC High Temperature Cement is high temperature resistant, highly thermal conductive and thermal shock resistant. In the surface temperature measurement problem, the contact in between the thermocouple and the surface of interest has been a big concern for investigators. First, if the contact is not sufficiently good, the air gap between the thermocouple and the surface of interest leads to uncertainties of temperature measurement because of the low thermal conductivity of air. Second, thermocouples cannot be located at a certain measuring point at the back surface of PMMA if the contact is not reliable. For instance, if the cement used does not survive a temperature of 400°C, the thermocouple is likely to move to a different measuring point after the cement melts. This surely results in invalid temperature measurements.

The cement used for this test functions sufficiently well so that reproducible temperature measurements are obtained. A representative data is shown in Figure 45.
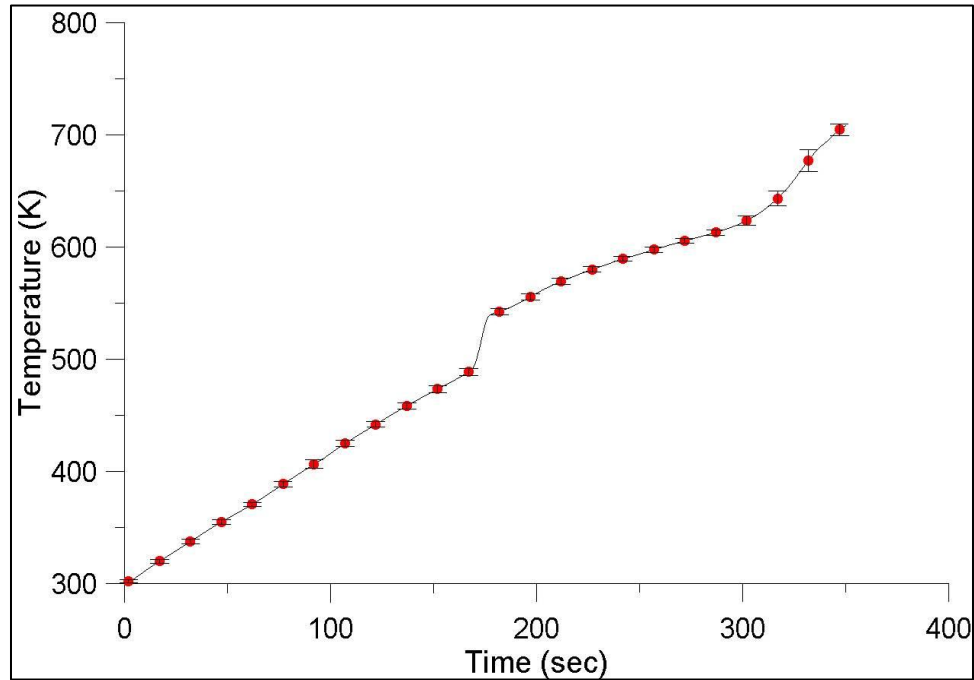
Several patterns should be noted in the temperature measurement and some hypotheses for the reason of these patterns are stated. 1). At around 180sec from the beginning of the test, these is a jump of temperature of about 50 K. This value of the temperature jump as well as the time of jump is repeatable in different temperature measurements. This jump of measurement is likely to result from the changes of contact between the aluminum foil and the PMMA sample. At the first 180 s of the gasification of PMMA, the PMMA is still solid at the bottom part. There must be some air in between the solid PMMA bottom and the aluminum foil. The low thermal conductivity leads to a relatively low temperature measurement. At around 180 s, the bottom of the PMMA sample finally turns to liquid phase after receiving enough energy from the cone heater. The liquid PMMA has a nice contact with the aluminum foil below and no air exist in between the sample and aluminum foil anymore. This causes the jump of the

temperature measurement. Since the air gap in the contact issue in surface temperature measurement is always a big concern, it is reasonable to guess that the temperature measurement after this jump is more accurate. 2). The time of the peak mass loss rate measurement is usually at around 280 sec from the beginning of the gasification test. From the observation, after this point, the liquid PMMA is usually not enough to cover the whole 80mm by 80mm sample area. Some part of the aluminum foil under the sample begins to receive heat flux directly from the cone heater then. Since the liquid PMMA is randomly distributed along the sample area in different tests, the measurement of temperature from this point becomes not as reproducible as the early stage of the measurement. 3). After the end of the gasification of PMMA, the temperature measurement goes up faster. This results from the fact that there is no more gasified PMMA carrying heat from the aluminum foil anymore. Furthermore, the whole aluminum foil begins to receive heat flux from the cone heater directly, leading to a faster temperature increase.

If all of these behaviors are taken into account, the most accurate temperature measurement is likely to be located at from 180 s to 280 s of the gasification of PMMA. In between this period of time, the liquid PMMA has perfect contact with the aluminum foil, leading to no contact issue for the surface temperature measurement. Moreover, the aluminum foil is not receiving heat flux directly from the cone heater, giving more accurate measurement of temperature of the back surface of PMMA sample. Thus, in the simulation of the back surface temperature, primary concentration is focused on whether the simulation can fit the measurement during this period of time.

4.3 ThermaKin Simulation Background

The one-dimensional Thermakin program is used in this study to simulate the back surface temperature of PMMA. The gasification MLR data of PMMA can also be obtained by ThermaKin simulation simultaneously. As discussed above, different thermal conductivity of PMMA is input into the model to give different back surface temperature. If the simulated temperature fits the experimental data, the corresponding thermal conductivity is regarded as the property of this material. Finally, verification of the predictive power of ThermaKin will be conducted by comparing the simulated gasification MLR with the experimental MLR measurement.

4.3.1 Input File of ThermaKin

Thermakin solves the non-steady energy and mass conservation equations accounting for chemical reactions described by a reaction mechanism. Two different files, a component file and a condition file, are included in the ThermaKin input files. The sample material is defined in Thermakin geometrically as a series of layers with specified thicknesses and chemically as material components defined by specific physical and chemical properties.

All these properties are defined in the component file. These properties include the density, heat capacity, thermal conductivity, mass transport coefficient, emissivity, and absorption coefficient. The emissivity and absorption coefficient are assumed constant for each component throughout the simulation. The other properties are defined as functions of temperature with the following equation where the property is generically denoted p:

$$p(T) = p_0 + p_1 T + p_n T^n \qquad (10)$$

Besides these properties, reactions are also described in the component file. The reaction occurs between one or two component and produced none to two components. Stoichiometry, Arrhenius reaction rate, heat of reaction and temperature limit of the reaction are also defined following the reaction equation.

In the condition file, first, the structure of the object is defined, including the thickness as well as the mass fraction of different component and the initial temperature of the component; second, the boundary conditions of object are defined. These include the top boundary and the bottom boundary. For each boundary, mass transport coefficient, outside temperature profile, convective coefficient, external radiation, absorption mode and the flame condition are defined. When the flame is off, the gasification test will be simulated. Other properties such like duration of simulation, element size and time step of simulation are also defined in the condition file.

Representative input files are provided in Appendix I – ThermaKin Input Files for Simulations of PMMA Gasification Test.

4.3.2 Absorption Mode

In ThermaKin, two different absorption modes – the maximum absorption algorithm (MAX) and the random absorption algorithm (RAND) – are defined. Either of these two modes is to determine the element that absorbs external radiation at every time step. In both cases, the external radiation is assumed to penetrate material in the direction normal to the boundary surface and behave in accordance with Beer-Lambert's Law [21]:

$$f^A = f^I a^A l^A \qquad (11)$$

Where f^I is the flux entering the element A, f^A is the flux absorbed by the element, a^A is the absorbance and l^A is the thickness of the element. When the maximum absorption algorithm is employed, the element that absorbs the most of the radiation is assumed to absorb all of it. In the other case where the random absorption algorithm is utilized, the absorbing element is selected at random using the Beer-Lambert distribution of absorbed energy as a probability density guiding this selection. In both cases, the absorbing element also acts as a gray body reflector and emitter.

The fact is that the optical properties, especially absorption coefficient of materials, are usually difficult to measure or estimate. In this study, first simulations are focused on the cases where the surface of the PMMA is assumed to be optically black. This is to see whether the simulations without taking into account the impact of optical properties can give satisfactory results. The radiant energy absorbed at the in-depth of PMMA is replaced by the conduction heat transfer into the material. It means that the absorption coefficient of the simulated material is assumed to be infinite high. The top element which is exposed directly to the external heat flux absorbs all of the energy. The energy transfer into the material is mainly by conduction. The in-depth of the simulated material does not receive any radiation heat flux from the heater, removing the impact of the absorption coefficient.

4.4 ThermaKin Simulation of Back surface Temperature and MLR – Regardless of Optical Properties

4.4.1 Simulation for Back surface Temperature of PMMA with h=15W/m^2*K

Simulations for the back surface temperature of PMMA are executed with all the properties either measured or assumed in previous discussions. Several chemical and thermal kinetic properties of PMMA are obtained by TGA/DSC measurements [22]. The convective coefficient is estimated to be 15W/m^2*K as analyzed in Section 3. The emissivity of PMMA is assumed to be 0.95 (as is commonly used in PMMA studies). The absorption coefficient of PMMA is assumes to be infinitely high, to assume that the PMMA is optically black. The thermal conductivity (k) is set to different values for a series of simulation to fit the experimental temperature measurement. With k=0.25 W/m*K and k=0.4 W/m*K, the comparison between the simulation and experiment are shown in Figure 46.
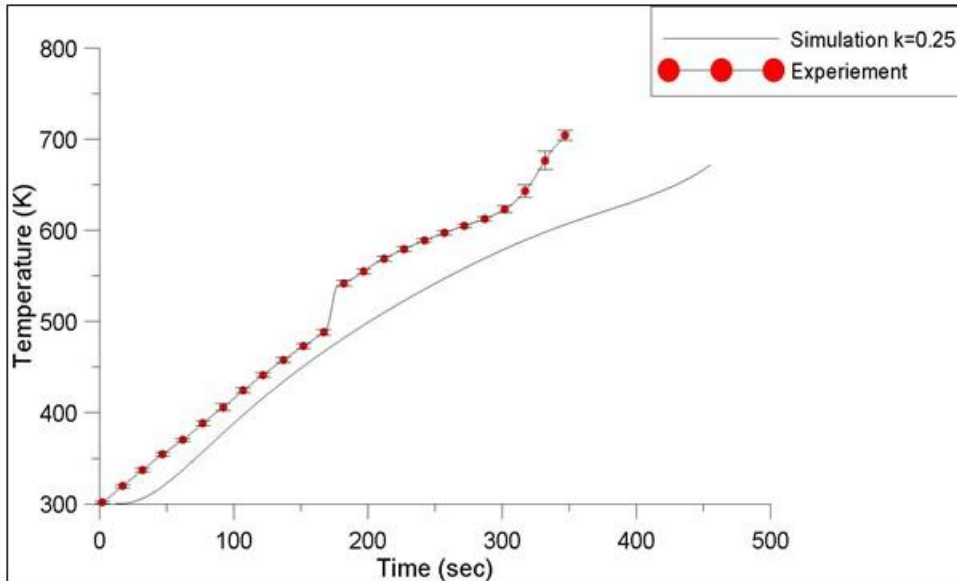
(a)
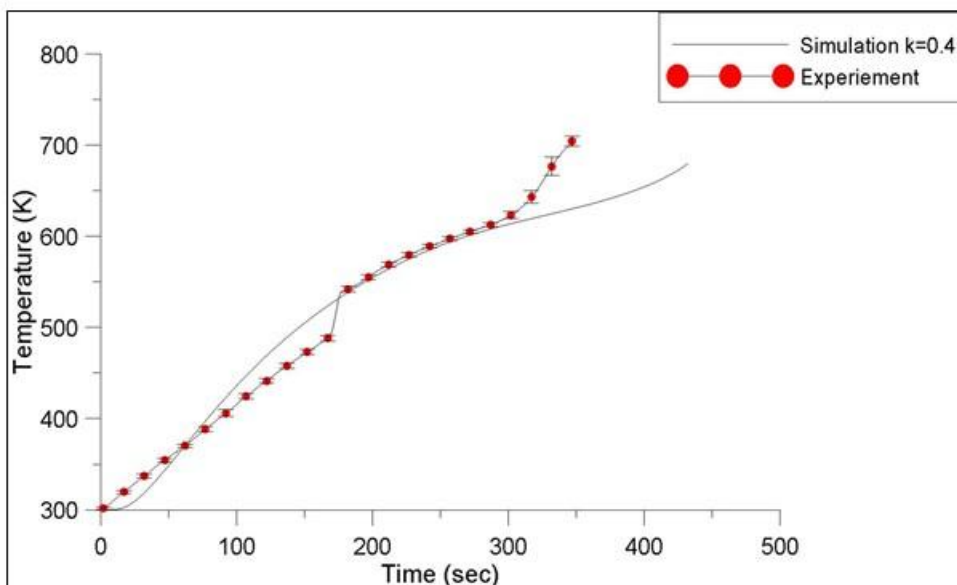
(b)

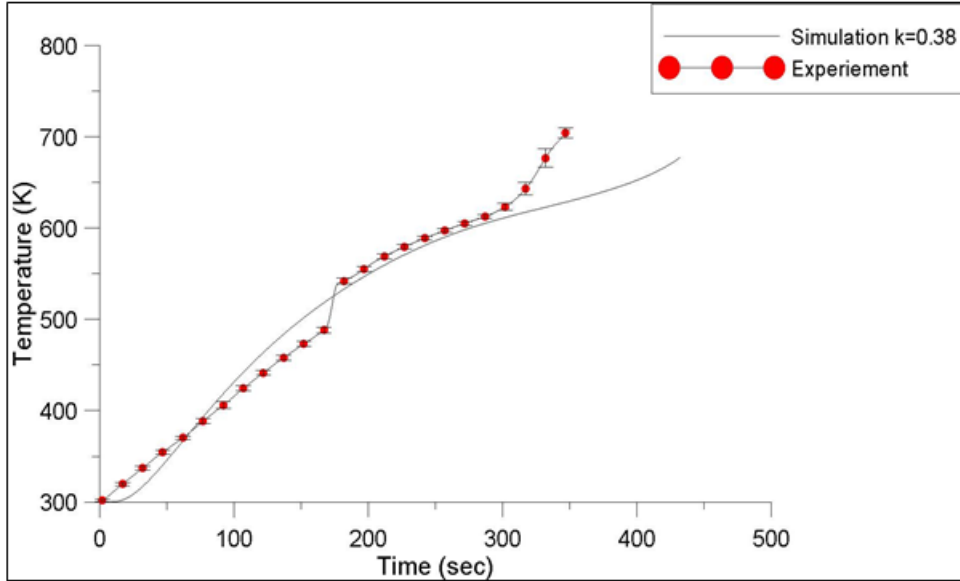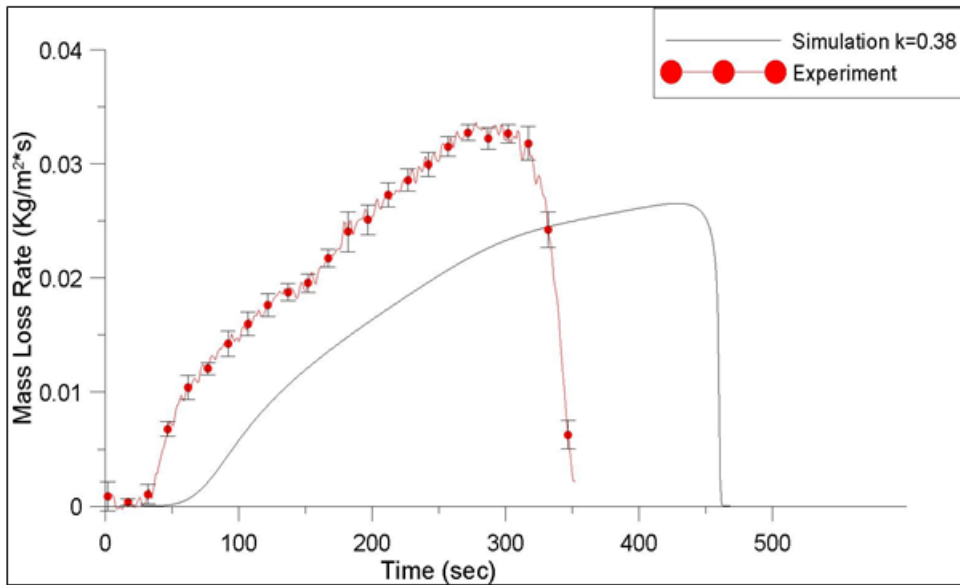Figure 46. 50 kW/m^2 - Comparison of PMMA Back surface Temperature between Experimental Measurements and Simulation, (a) k=0.25 W/m*K (b) k=0.4 W/m*K, α=100 m^2/kg, ε=0.95

When k=0.25 W/m*K, the simulated temperature is lower than the experimental data. It means the k value is not high enough for energy to transfer through the simulated PMMA. However, when the k is raised to 0.4 W/m*K, the simulated

temperature appears to be a little higher than the experimental data. It means a lower k

is needed for a better fit.

(a)

(b)

Figure 47. 50 kW/m^2 - Comparison of Back surface Temperature of PMMA (a) and Gasification MLR (b) between Simulation and Experiment, h=15 W/m^2*K, k=0.38 W/m*K, α=100 m^2/kg, ε=0.95

Then thermal conductivity of PMMA is defined as 0.38 W/m*K in the ThermaKin simulation input file, the back surface temperature of PMMA as well as the gasification mass loss rate profiles are compared with the experimental data in Figure 47.The simulated back surface temperature of PMMA is able to fit the experimental temperature measurement excellently. Nevertheless, the gasification MLR data does not agree with each other. The simulated gasification MLR is significantly slower than the experimental one.

4.4.2 Analysis of the Convective Boundary Layer

The disagreement between the simulated and experimental MLR is significant as shown in Figure 47 (b), even if the simulation of back surface temperature of PMMA is excellent. In the simulation, the radiant heat flux, re-radiation is regarded as well defined. Another possible difference between the simulation and experiment seems to be the convective heat loss.

As discussed in Chapter 2 and Chapter 3, the method of estimating the convective coefficient is to simulate the copper temperature in the gasification environment. The copper is high temperature resistant thus it does not produce any products during the tests. However, In the CAPA gasification experiments for polymers, it is observed that a lot of gasification products are being pushed up to the cone heater from the sample being gasified. These products consist of some visible smoke and some invisible gases of a temperature estimated to be around 600K. The products are directed upward so violently that the convective boundary layer is believed to be changed by this blowing effect. But, the convective coefficient estimated by the copper test is the one when the convective boundary layer does exist above the copper. If it is the truth, then the convective coefficient of 15 W/m^2*K should be over-estimated for the polymer gasification tests. A convective coefficient of 0 W/m^2*K is input into the ThermaKin of simulation to see whether this hypothesis is right.

4.4.3 Simulation for Back surface Temperature of PMMA with h=0 W/m^2*K

(a)

(b)

Figure 48. 50 kW/m^2 - Comparison of Back surface Temperature of PMMA (a) and Gasification MLR (b) between Simulation and Experiment, h=0 W/m^2*K, k=0.33 W/m*K, α=100 m^2/kg, ε=0.95
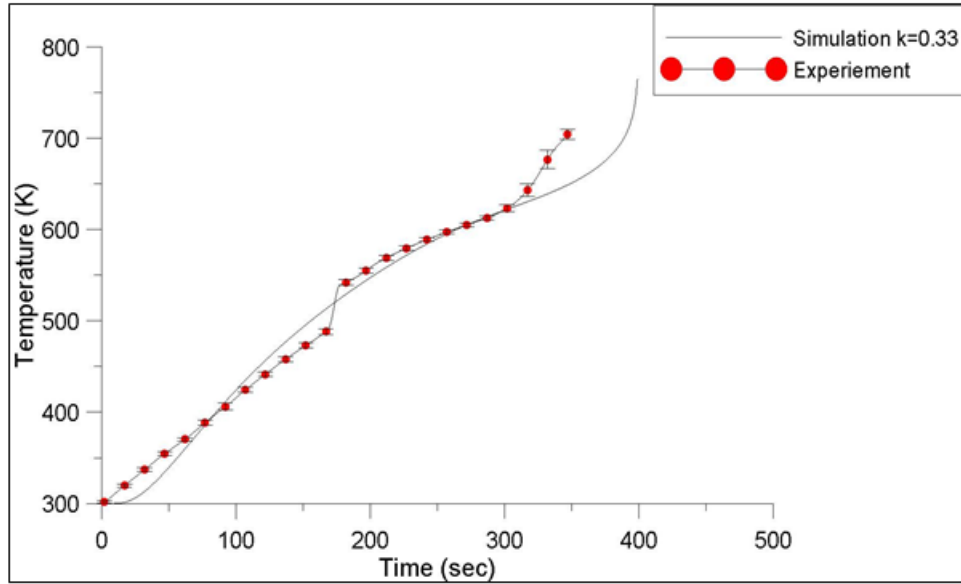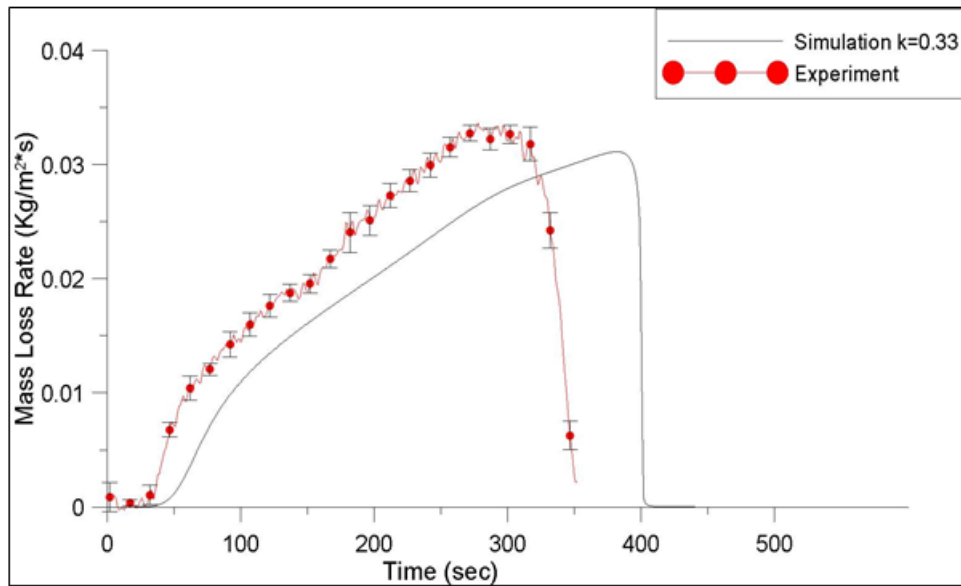
Similar steps as taken in Section 4.4.1 are followed in this section. After different tries of different thermal conductivity values, k=0.33 W/m*K could give the best fit of back surface temperature of PMMA as seen in Figure 48 (a).

The simulated and experimental gasification mass loss rate profiles are compared in Figure 48 (b) with the premium k for temperature fitting. These two MLR profiles are much closer to each other than the case in Section 4.4.1. The peak values are much closer to each other than the previous case. This could demonstrate that the hypothesis stated in Section 4.4.2 about the destroyed convective boundary layer is reasonable..

Although the simulation has been improved, the agreement between the MLR profiles is still not satisfactory. The reason is that, in these cases, the impact of optical properties are eliminated by means of giving a large absorption coefficient of PMMA and setting the absorption mode to be MAX. To improve the simulation, more realistic optical properties are taken into account. With a absorption coefficient obtained from a recent study and absorption mode of RAND, the in-depth PMMA will be able to receive the radiant heat flux from the cone heater. Higher energy into the simulated material can surely lead to a faster thus closer gasification MLR simulation.

4.5 ThermaKin Simulation of Back surface Temperature and MLR – With Consideration of Optical Properties

To take the optical properties into account, first of all, the absorption mode should be RAND. Secondly, the emissivity and absorption coefficient should be found in literature. In a recent work by Linteris et al [23], several popular polymers including clear PMMA were well studied to measure the emissivity and absorption coefficient. The emissivity of clear PMMA was measured to be 0.96 while the absorption coefficient

was 2.08. These two important optical properties for PMMA are then input into the

ThermaKin simulation to see whether the simulation could be improved.

First, absorption and emissivity data from literature, the measured convective
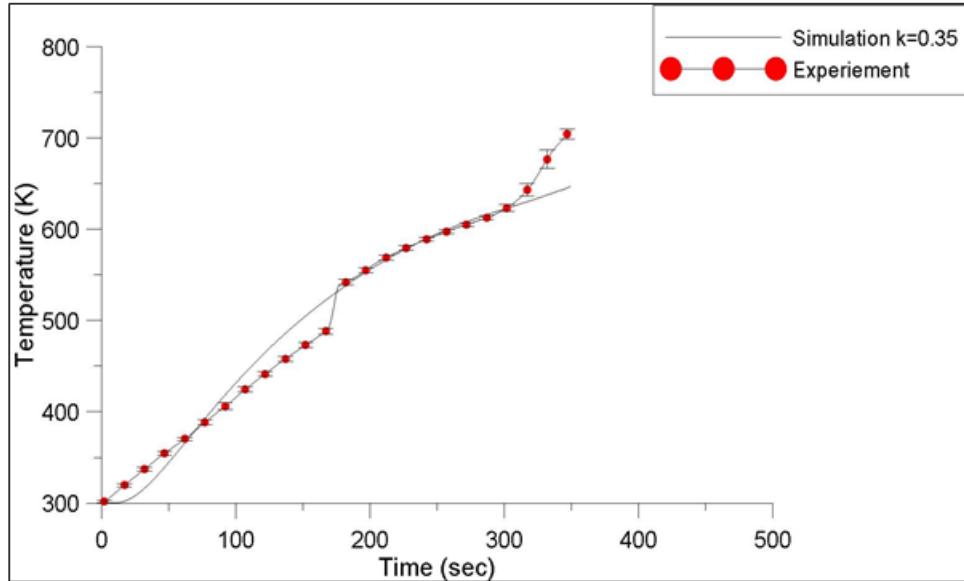
(a)
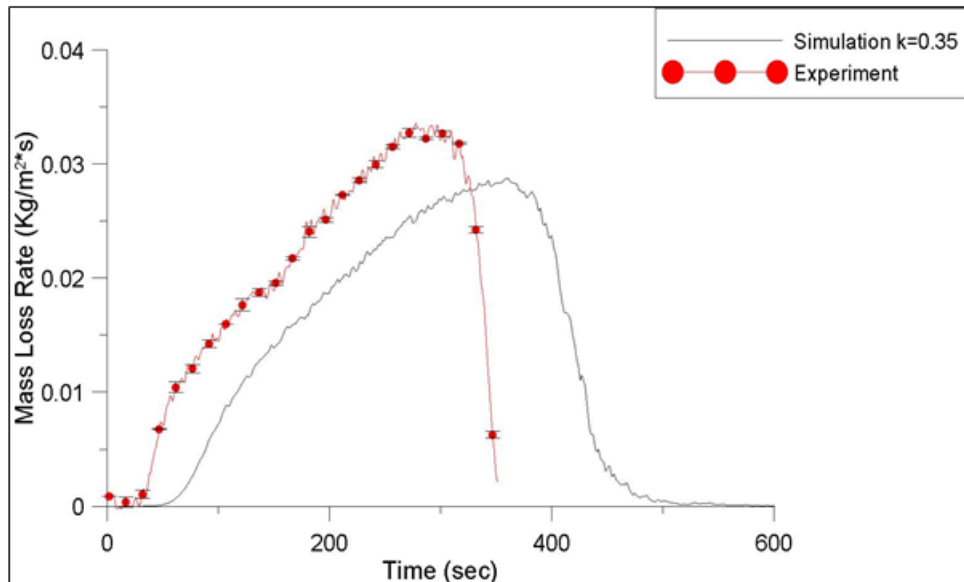
(b)

Figure 49. 50 kW/m^2 - Comparison of Back surface Temperature of PMMA (a) and Gasification MLR (b) between Simulation and Experiment, h=15 W/m^2*K, k=0.35 W/m*K, α=2.08 m^2/kg, ε=0.96

coefficient h=15W/m^2*K are used in the simulations. When the thermal conductivity of PMMA is set 0.35W/m*K, the best fit of back temperature of PMMA is obtained. The data and the corresponding gasification MLR are shown in Figure 49. The simulation is still relatively lower than the experimental data. This could also demonstrate that convective coefficient of 15 W/m^2*K is too high.

Second, since the convective boundary layer is likely to be altered during the gasification of polymers as discussed in Section 4.4.2, here in these simulations, the convective coefficient is also defined as 0 W/m^2*K. Followed by the steps in the previous procedure of simulation and fitting, the simulation of back surface temperature of PMMA can fit the experimental measurement when thermal conductivity k=0.25W/m*K. The temperature profiles and the corresponding gasification MLR profiles can be seen in Figure 50.

The agreement between the simulation and experiment of the temperature as well as the gasification mass loss rate is excellent. For this closest comparison seen in Figure 50, the peak and average mass loss rate obtained from the simulations are only respectively 6% and 11% lower than the corresponding experimental data.

Potential sources of the discrepancies are analyzed including the effects of uncertainties of material properties in the ThermaKin input file. 1). The convective coefficient is assumed to be 0 W/m^2*K, based on the conclusion that the convective boundary layer is destroyed by the blowing effect of the products of gasified PMMA. However, in the experiment, the blowing effect may not be able to remove all the convective heat loss from the surface. But it is still hard to quantify the h value. 2). The

thermal conductivity, emissivity and absorption coefficient are all assumed to be constant values in the simulation. It is very likely that all these properties are temperature dependent; the optical properties are also likely to be spectrum dependent.
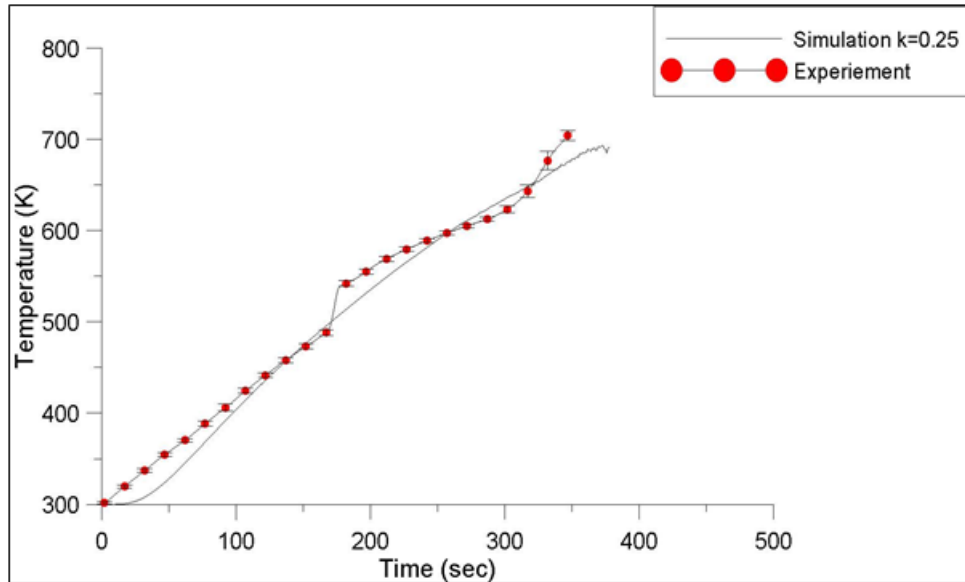
(a)
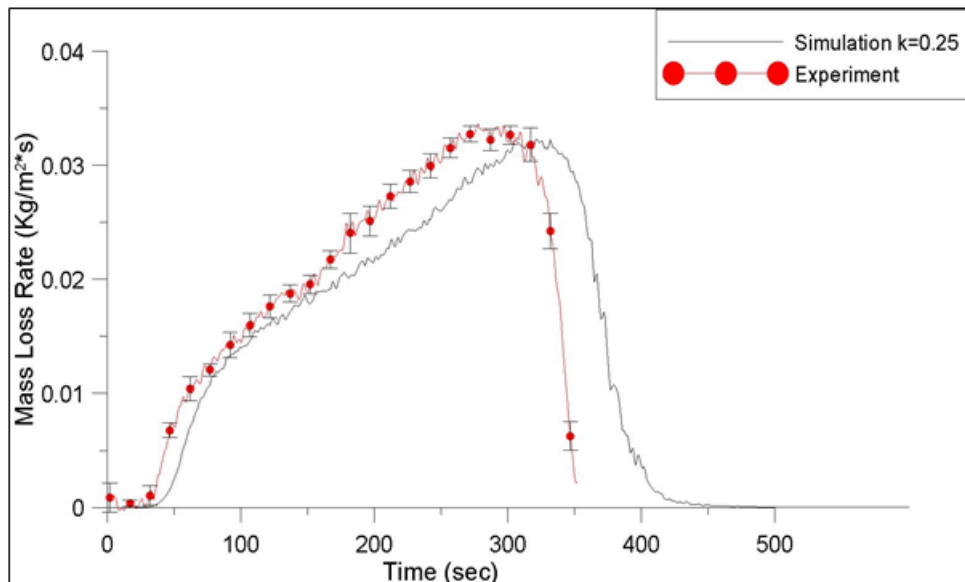
(b)

Figure 50. 50 kW/m^2 - Comparison of Back surface Temperature of PMMA (a) and Gasification MLR (b) between Simulation and Experiment, h=0 W/m^2*K, k=0.25 W/m*K, α=2.08 m^2/kg, ε=0.96

4.6 Further Verification of ThermaKin Simulation – 35kW/m^2 of External Heat Flux

With external heat flux of 50kW/m^2 from the cone heater, the thermal conductivity of PMMA is estimated under different assumptions of the material properties. The predictions by ThermaKin are proved to be excellent. To verify the predictive power of ThermaKin one more step forward, all the assumptions of material properties and the corresponding k value obtained in the last section are utilized for the PMMA gasification MLR simulations under 35kW/m^2 of external heat flux.

1). With convective coefficient of 15W/m^2*K in the boundary condition, infinitely large absorption coefficient, emissivity coefficient of 0.95 and thermal conductivity of 0.38W/m*K for the PMMA. Under 35kW/m^2, the comparison of simulated gasification MLR to the experimental data is shown in Figure 51.

Figure 51. 35kW/m^2 - Comparison of Gasification MLR of PMMA between Simulation and Experiment, h=15 W/m^2*K, k=0.38 W/m*K, α=100 m^2/kg, ε=0.95

2). With convective coefficient of 0W/m^2*K in the boundary condition, infinitely large absorption coefficient, emissivity coefficient of 0.95 and thermal

conductivity of 0.33W/m*K for the PMMA. Under 35kW/m^2, the comparison of simulated gasification MLR to the experimental data is shown in Figure 52.

Figure 52. 35kW/m^2 - Comparison of Gasification MLR of PMMA between Simulation and Experiment, h=0 W/m^2*K, k=0.33 W/m*K, α=100 m^2/kg, ε=0.95

Figure 53. 35kW/m^2 - Comparison of Gasification MLR of PMMA between Simulation and Experiment, h=15 W/m^2*K, k=0.35 W/m*K, α=2.08 m^2/kg, ε=0.96

3). With convective coefficient of 0W/m^2*K in the boundary condition, absorption coefficient of 2.08 m^2/kg, emissivity coefficient of 0.96 and thermal conductivity of 0.25W/m*K for the PMMA. Under 35kW/m^2, the comparison of simulated gasification MLR to the experimental data is shown in Figure 53.
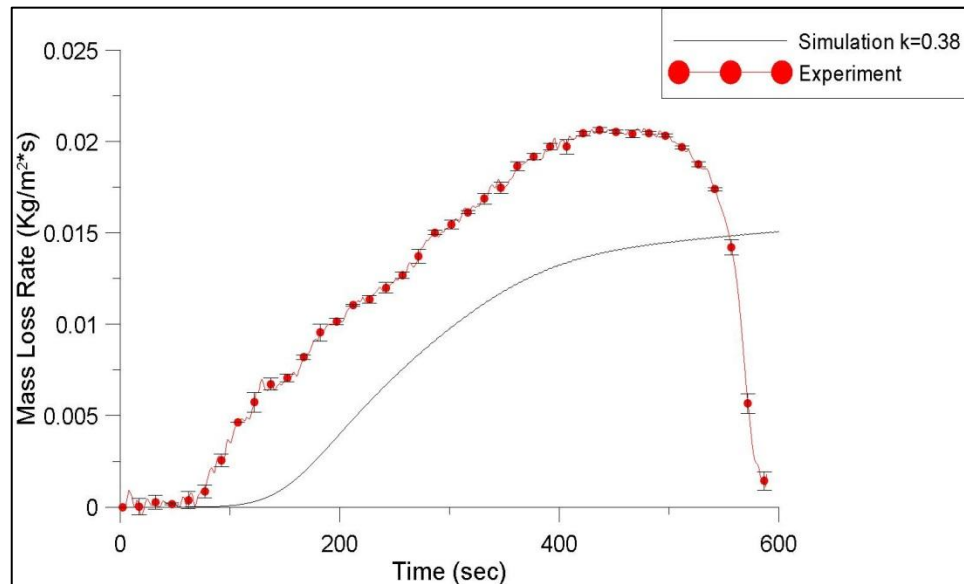
4). With convective coefficient of 0W/m^2*K in the boundary condition, absorption coefficient of 2.08 m^2/kg, emissivity coefficient of 0.96 and thermal conductivity of 0.25W/m*K for the PMMA. Under 35kW/m^2, the comparison of simulated gasification MLR to the experimental data is shown in Figure 54.

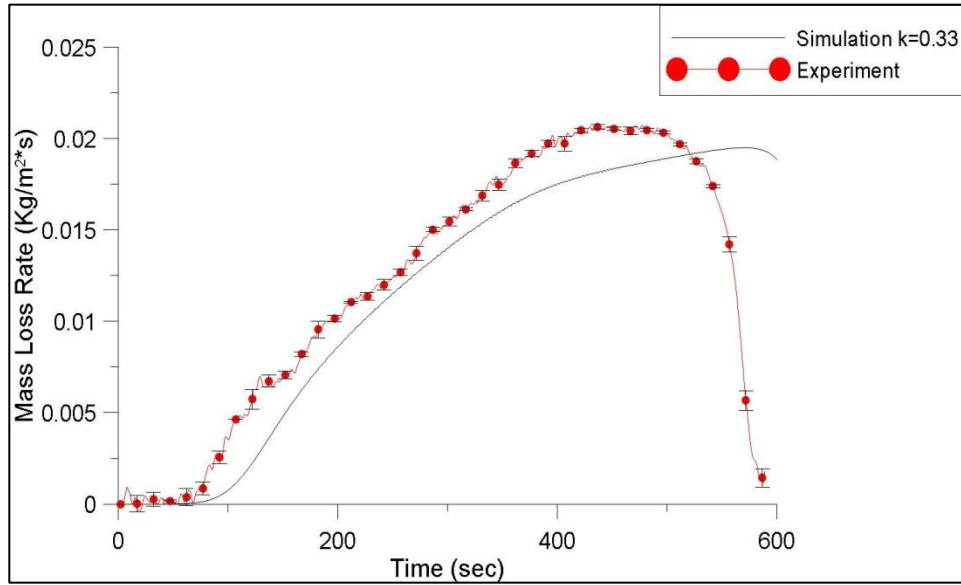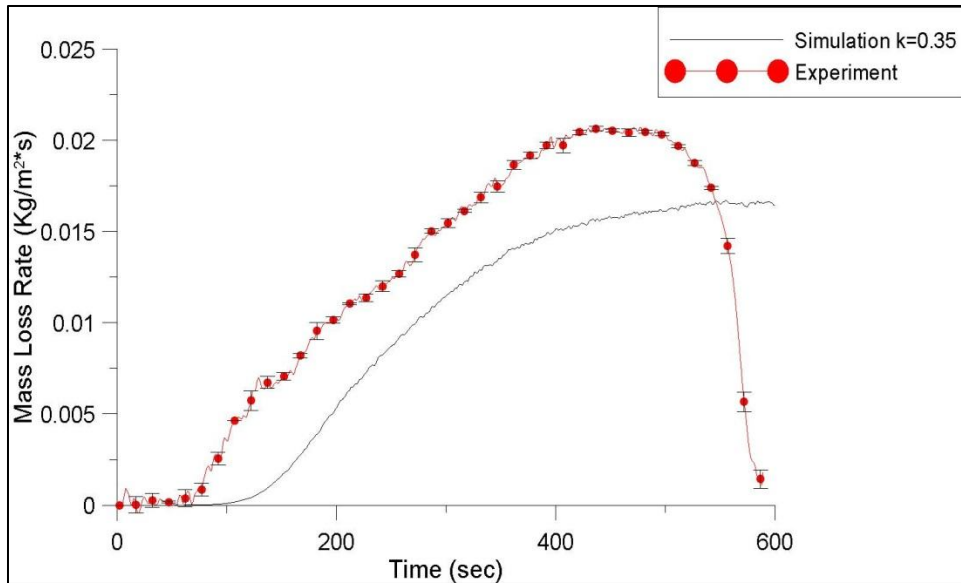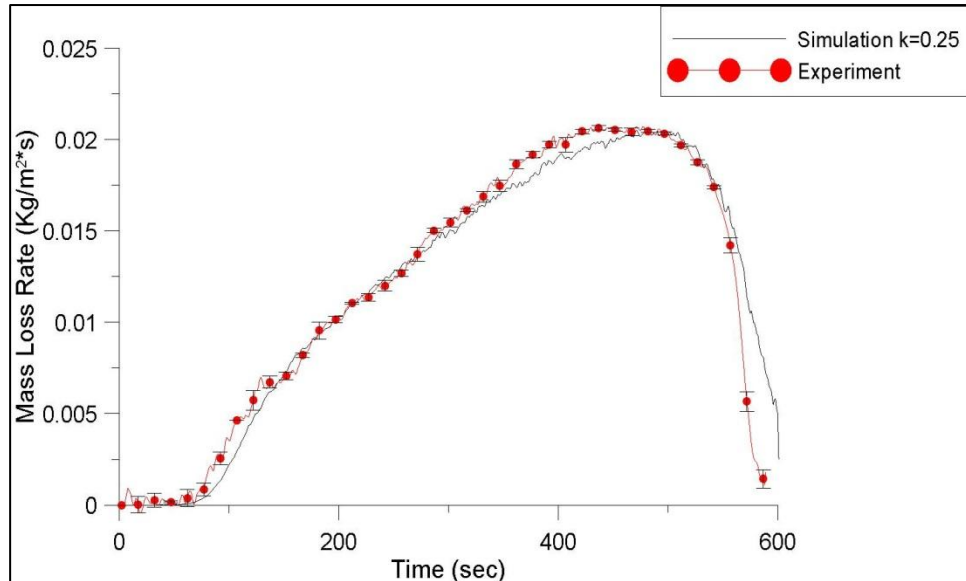**Figure 54. 35kW/m^2 - Comparison of Gasification MLR of PMMA between Simulation and Experiment, h=0 W/m^2*K, k=0.25 W/m*K, α=2.08 m^2/kg, ε=0.96**

In the first situation, the simulated MLR is much lower than the experimental data, while in the second and third situation, the simulated MLR is much better compared to the first simulation. However, in the last situation, the simulation and the experiment agree with each other almost perfectly. When the heat flux is 50kW/m^2,

the simulation also has excellent agreement with the experiment as discussed in Section 4.5.

It can be seen from both 50 kW/m^2 and 35 kW/m^2 cases that, if the PMMA is regarded as optically black and the potential deviations in the experiments are taken into account, the estimated thermal conductivities are sufficiently reasonable and the gasification mass loss rate simulations have good agreement with the experimental data. If the optical properties are also taken into account, the thermal conductivity estimated looks more reasonable compared to some literature data. The gasification mass loss rate simulations have excellent agreement with the experimental data.

5. Conclusion

At this point, several important conclusions could be safely drawn:

1). It is possible to achieve a low oxygen concentration environment for gasification experiments in the open atmosphere at a standard cone calorimeter. Two versions of design are employed and analyzed – The "Nitrogen Frame" and "CAPA".

2). The gasification environment by "Nitrogen Frame" is well understood and all the influencing factors except for the oxidation factor are quantified. The oxidation factor in this design is hard to quantify as well as to eliminate.

3). The oxidation factor has minor impact on the gasification process of PMMA, but it increases the gasification rate of PP significantly.

4). The second version of the gasification apparatus design - Controlled Atmosphere Pyrolysis Apparaus "CAPA" – is able to reduce the oxygen concentration at the sample tremendously. (3.1% when the nitrogen flow rate is 200SLPM).

5). The convective coefficient in both designs is able to be quantified by means of fitting the simulated copper temperature data to the experimental values. This coefficient is estimated to be 50W/m^2*K in "Nitrogen Frame" and 15W/m^2*K in CAPA.

6). In the CAPA design, if the bottom opening is not enclosed, heat flux will result in significant amount of air coming from the bottom during the gasification tests, resulting in much higher oxygen concentration at the sample. The enclosed bottom of CAPA could largely reduce the oxygen concentration under different heat fluxes.

7). The back surface temperature of PMMA is able to be reproducibly measured. By fitting the simulated temperature profiles with the experimental data, reasonable thermal conductivity of PMMA could be estimated.

8). With all the properties of PMMA including the thermal conductivity measured in this study, ThermaKin is able to predict the gasification MLR of PMMA under 35kW/m^2 and 50kW/m^2 with excellent agreements to the experimental values. Therefore, the thermal conductivity of PMMA is determined to be 0.25W/m*K. Furthermore, the predictive power of ThermaKin could be verified.

9). Without taking into account the optical properties of PMMA, satisfactory gasification mass loss rate is able to be simulated. With the optical properties, the simulation is even better. It is likely that the optical properties are playing important role in the prediction of gasification mass loss rate.

10). In all the gasification MLR simulations, the convective coefficient is assumed to be 0W/m^2*K because that the convective boundary layer is likely to be altered by the blowing effect of gasification products.

5.1 Future Work

Extension of this study will be focused on PolyPropylene (PP) to estimate the thermal conductivity and to predict the gasification mass loss rate by ThermaKin. Similar studies will be concentrated on other non-charring and charring materials.

A parallel study will be conducted with CAPA to investigate the oxygen effect on testing materials such as card board.

Appendix I – ThermaKin Input Files for Simulations of PMMA Gasification Tests.

Representative input files for ThermaKin simulation of the back surface temperature of

PMMA as well as the gasification mass loss rate are listed here. They include the

component file (pmma.cmp) and the condition file (pmma.cnd). By these files, the

simulation of best agreement with the experimental data (discussed in Section 4.5)

could be obtained.

Component File:
pmma.cmp
COMPONENT: KAOWOOL
STATE: S
DENSITY: 240 0 0 0
HEAT CAPACITY: 1070 0 0 0
CONDUCTIVITY: 0.0519 -4e-5 1e-7 2
TRANSPORT: 1e-30 0 0 0
EMISSIVITY & ABSORPTION: 0 1000

COMPONENT: PMMA
STATE: S
DENSITY: 1154 0 0 0
HEAT CAPACITY: 601.4 3.63 0 0
CONDUCTIVITY: 0.25 0 0 0
TRANSPORT: 1e-5 0 0 0
EMISSIVITY & ABSORPTION: 0.96 2.08

COMPONENT: PMMA_g
STATE: G
DENSITY: 1154 0 0 0
HEAT CAPACITY: 601.4 3.63 0 0
CONDUCTIVITY: 0.25 0 0 0
TRANSPORT: 1e-5 0 0 0
EMISSIVITY & ABSORPTION: 0.96 2.08

MIXTURES
S SWELLING: 0
L SWELLING: 0

G SWELLING LIMIT: 1e-30
PARALL CONDUCTIVITY: 0.5
PARALL TRANSPORT: 0.5

REACTION: PMMA + NOCOMP -> NONCOMP + PMMA_g
STOICHIOMETRY: 1   0   0   1
ARRHENIUS: 8.6e12 188100
HEAT: -892900 0 0 0
TEMP LIMIT: L 300

Condition File:
pmma.cnd
OBJECT TYPE: 1D

OBJECT STRUCTURE
****

THICKNESS: 0.00635
TEMPERATURE: 300
MASS FRACTIONS:
PMMA 1

THICKNESS: 0.01600
TEMPERATURE: 300
MASS FRACTIONS:
KAOWOOL   1

OBJECT BOUNDARIES
****

TOP BOUNDARY

MASS TRANSPORT: YES
PMMA_g LIN 0.05 0

OUTSIDE TEMP TIME PROG: 300 0
CONVECTION COEFF: 0

EXTERNAL RADIATION: YES
TIME PROG1: 5e4 0 6e2

TIME PROG2: 0   0 0
REPEAT: NO
ABSORPTION MODE: RAND

FLAME: NO

BOTTOM BOUNDARY

MASS TRANSPORT: NO

OUTSIDE TEMP TIME PROG: 300 0
CONVECTION COEFF: 0

EXTERNAL RADIATION: NO

FLAME: NO

INTEGRATION PARAMETERS
****

ELEMENT SIZE: 5e-5
TIME STEP: 0.01
DURATION: 600

OUTPUT FREQUENCY:
ELEMENTS: 1
TIME STEPS: 100

Reference

1. Babrauskas, V., *Development of the Cone Calorimeter: A Bench-Scale Heat Release Rate Apparatus Based on Oxygen Consumption.* NBSIR 82-2611, 1982.
2. *ASTM E 1354-09: Standard Test Method for Heat and Visible Smoke Release Rates for Materials and Products Using an Oxygen Consumption Calorimeter.* American Society for Testing and Materials, Philadelphia, PA., 1990.
3. *ISO 5660: International Standard -Fire Tests -Reaction to Fire -Rate of Heat Release from Building Products.* International Organization for Standards, Geneva.
4. Mulholland, G., et al., *The effect of Oxygen Concentration on CO and Smoke Produced by Flames.* Proceeding of the Third International Symposium of Fire Safety Science, Edimburg UK, 1991: p. 585-594.
5. Babrauskas, V., et al., *A Cone Calorimeter for Controlled Atmosphere Studies.* Fire and Material, 1992(16): p. 37-43.
6. Petrella, R.V. and N. Batho, *The Controlled-Atmosphere Cone Calorimeter - an Improved tool for Fire Testing of Materials.* Proceeding of the 1st International Conference Fire and Materials, San Francisco, USA, 1992: p. 311-321.
7. Hshieh, F.Y., et al., *Flammability Testing using a Contrlled-Atmosphere Cone Calorimeter.* Proceeding of the 18th International Conference on Fire Safety, Millbrae CA, USA, 1993: p. 999.
8. Hshieh, F.Y. and R.R. Buch, *Controlled Atmosphere Cone Calorimeter Studies of Silicones.* Fire and Material, 1997(21(6)).
9. Hietaniemi, J., R.Kallonen, and E.Mikkola, *Burning Characteristics of Selected Substances: Production of Heat, Smoke and Chemical Species.* Fire and Material, 1999(23): p. 171-185.
10. V.P.Dowling, J.E. Leonard, and P. Bowditch, *Use of a Controlled Atmosphere Cone Calorimeter to Asses Building Materials.* Proceeding of the 8th International Conference Fire Science, 1999: p. 989-997.
11. G.J.Griffin, A.Bicenell, and T.J.Brown, *Studies on the Effect of Atmospheric Oxygen Content on the Thermal Resistance of Instumescent, Fire Retardant Coating.* Journal of Fire Science, 2005(23(4)): p. 303-328.
12. Leonard, J.E., P.A. Bowditch, and V.P.Dowling, *Development of a Controlled-atmosphere Cone Calorimeter.* Fire and Material, 2000(Fire Mater. 24): p. 143-150.
13. Kashiwagi, T., A. Omori, and H. Nanbu, *Effects of Melt Viscosity and Thermal Stability on Polymer Gasification.* Combustion and Flame, 1990(81): p. 188-201.
14. Kashiwagi, T. and T.J. Ohlemiller, *A Study of Oxygen Effects on Non-flaming Transient Gasification of PMMA and PE During Thermal Irradiation.* Nineteenth Symposium (International) on Combustion/ The combustion Insititute, 1982: p. 815-823.
15. Austin, P.J., R.R. Buch, and T. Kashiwagi, *Gasification of Silicone Fluids Under External Thermal Radiation.* NISTIR 6041, 1997.

16. Austin, P.J., R.R. Buch, and T. Kashiwagi, *Gasification of Silicone Fluids under External Thermal Radiation Part 1. Gasification Rate and Global Heat of Gasification.* Fire and Material, 1998(22): p. 221-237.

17. *ASTM E 2058-09: Standard Test Methods for Measurement of Synthetic Polymer Material Flammability using a Fire Propagation Apparatus (FPA).* American Society for Testing and Materials, Philadelphia, PA.

18. Stoliarov, S.I. and R.E. Lyon, *Thermo-Kinectic Model of Burning.* Atlantic City: Federal Aviation Administration, 2008.

19. Stoliarov, S.I., et al., *Prediction of the Burning Rates of Non-Charring Polymers.* Combustion and Flame, 2009(156): p. 1068-1083.

20. Stoliarov, S.I., et al., *Prediction of the Burning Rates of Charring Polymers.* Combustion and Flame, 2010(157): p. 2024-2034.

21. Atkins, P.W., Physical Chemistry, 1978(W.H. Freeman and Company, San Francisco, CA, USA): p. 582-611.

22. Stoliarov, S.I., et al., *Measurement of the Thermodynamics of Polymers Degradation.* 6th Fire and Polymers Symposium, 243rd ACS National Meeting p. 44.

23. Linteris, G., et al., *Absorption and Reflection of Infrared Radiation by Polymers in Fire-like Environment.* Fire and Material, 2011(2011): p. 1-12.